Innovative Approaches for Flood Risk Management and Financing in Agriculture

A Sub-paper on: "International Review of Flood Risk, Flood Modeling and Flood Mapping to Support Flood Insurance in Agriculture"

G. Robert Brakenridge
Research Associate Professor
Department of Geography
Dartmouth College
Hanover, NH 03755 USA

Introduction 1
Previous work 2
Contemporary Techniques for Flood Risk Assessments 3
Overview 3
Wide-Area Flood Risk Mapping 5
Traditional Risk Assessment and the Assumption of Stationarity 7
Remote Sensing Resources for Flood Risk Mapping 10
New Strategies for Flood Risk Mapping and Determination of Flood Indices 16
Types of Flood Risk and the Design of Flood Damage Indices 22
Summary and Conclusions 29
References Cited 29

Introduction

This paper provides technical information needed to support index-based flood insurance solutions, which rely heavily on objective loss adjustments. Such "contingent claims" contracts can be determined by objective parameters such as flood height (stage), flood area (within specified floodplains), peak discharge, duration, and so forth: parameters that strongly correlate to actual losses and revenue outcomes. Index-based contracts reduce administrative costs and provide for timely payouts, and are most suitable when applied to co-variate risks affecting large groups of people or over large regions. They have been used previously for losses from drought, which causes significant crop losses but is otherwise difficult to insure by traditional methods. Beginning in 2003, the use of rainfall-index insurance contracts for drought risk management was piloted by the World Bank and partners in, for example, India, Malawi, and Ethiopia. Farmers who are protected by index contracts receive timely payouts when the compensation is automatically triggered: when the chosen index parameter reaches a pre-specified level. The automatic trigger reduces administrative costs for the insurer by eliminating the need for field-level damage assessment. The World Bank now seeks practical and efficient methods to implement such index-based insurance for losses from coastal and inland flooding.

The Commodity Risk Management Group (CRMG) of the World Bank is working to scale up the existing index insurance projects for new client countries and for new risks. Given the importance of flood risks in Asia, Africa, Central America, and many other parts of the developing world, CRMG seeks methods to index flood losses. Extending the index approach from drought risk to flood risk requires the Group to expand into new technologies. For example, whereas the drought indexes can be constructed with rainfall data using relatively established methodology, the more-varied causation of flood damage may require using a combination of data sources, including river gage and rainfall data, flood modeling, agro-meteorological modeling, and satellite images (remote sensing). These may be needed in order to design flood indexes that accurately estimate crop losses, and also to assess flood hazard prior to any event.

Feasibility studies and technical development work for flood index insurance are being undertaken in Thailand, Vietnam (SIWRP, 2006) and Bangladesh at the present time, and are expected to lead to pilot projects.

Previous work

In November 2005, CRMG contracted a team of experts led by PASCO Corporation, Japan, to develop a prototype flood index for rice production in the Pasak Basin in Phetchabun, Thailand. The study was completed in July 2006 and resulted in an index which quantifies the impact of flood duration and depth on rice yield loss during the flowering and pre-harvest time window (PASCO, 2006). Based on the flood index, it is proposed that farmers will start receiving incremental insurance payouts after 4 days of inundation and total sum insured after 7 days. In order to operate the insurance scheme, a GIS (Geographical Information Systems) database must be created for the pilot area. When rice production reaches the critical period, satellite images will be continuously captured and analyzed in relation to the GIS database to determine whether a flood event of payout-triggering duration has occurred.

The primary limitations identified are: (1) insufficient quality of topographic and hydro-meteorological data to parameterize and validate the chosen flood model; and (2) the chosen modeling approach, which is computationally too expensive to generate sufficient time series of outputs for the purpose of actuarial pricing. Additional information is also needed with regards to farming practices, flood regime and management, and socio-economic impacts of flood on rice farmers in order for an appropriate flood insurance scheme to be designed.

Several technologies are now being applied to further develop index-based flood insurance. These include: 1) *GIS and related information-processing technologies*, 2) *flood modeling* (here the term includes both runoff modeling, which predicts the size and duration of flood discharge from meteorological information, and hydraulic or hydrodynamic modeling, which predicts the heights and durations reached by flood waves of known size traveling along the floodplain), 3) *orbital remote sensing* of actual flooding, and 4) *agro-meteorological* modeling that analyzes flood-related crop damage. In regard to these technologies, remote sensing is a vital operational tool for loss assessments, as it enables the detection of actual flooded areas. If farmers are enrolled for insurance within a GIS-linked database, rapid detection of the location, areal extent, and duration of flooded fields becomes a possibility given an adequate quantity of applicable remote sensing data. However, and depending on the quality and quantity of the remote sensing, flood modeling may be needed to extend geographically and though time the inundation observations. Thus, a satellite may capture information at high spatial resolution but separated days and perhaps even weeks in time, and there may remain the need to objectively map the maximum inundation limit, even if the satellite missed the actual peak. Finally, a cornerstone of this insurance approach is for loss assessment to be carried out in an objective, independent and low cost manner. Agro-meteorological modeling, coupled with flood modeling, can help construct a simplified indexed flood insurance product, where agreed payouts are matched to damage expected from specific meteorological events.

Insurance underwriting also requires that information is available to enable spatial allocation of farmers into specified homogenous risk zones where estimates of the probable *frequency* and *severity* of flooding can be made. Flood modeling, coupled with the remote sensing and the ground station-based record of past events, is an appropriate technique for identifying flood zones and for estimating the *return period of expected flooding*. Such is needed for the purposes of premium calculation, according to the product designed for that crop. Generally, flood information is required within specific *flood windows* (time periods) that relate to crop growth stages. The challenge is to harness new, objective data-producing technologies, models, and data analysis techniques to risk assessment, as well as to loss payment procedures.

Prior to the present report, CRMG reached some preliminary conclusions. These are that: 1) *Flood types*, as well as the types of *flood catchments and basins*, (e.g. mountain watershed flash floods, coastal storm surge floods, tropical cyclone-induced inland flooding) strongly affect the feasibility of flood index insurance. Thus, it is important that these types of flood risk be categorized and reviewed from an international and regional perspective, in regard to their relative importance for agricultural damage amounts, and in order to develop the most appropriate indices to trigger loss payouts. 2) *Flood risk modeling* is a well-developed technique, in wide but exceptionally varied use internationally. If flood index insurance is to be commonly applied, however, it may be necessary to support continued progress and innovation in the techniques used to develop flood risk zones and estimate hazard exposure. Finally, 3) Unlike the case for drought, even minor on-the-ground land cover or river way modifications can alter the downstream flood risk. Therefore, it is essential that provision be made for *updating of geospatial data* such that land areas newly protected from flooding, or newly at risk, can be identified in a timely manner.

There are two different but inter-related needs: 1) objective assignment of land parcels and crops into flood risk zones, and 2) consistent and accountable determination, as floods occur, of local exceedance of flood index threshold values; such that reliable prediction can be made of crop losses without intensive field verification. The present report summarizes current techniques for flood risk assessment, and analyzes the variety of flood risks from different genetic classes of floods, and including the different methods that are appropriate for analyzing risk. It then presents the contributions that can be made by the various geospatial technologies listed above and describes their appropriate roles and limitations. Finally, it considers how the same and other technologies can be incorporated into flood index design, and illustrates though specific examples the production of reliable predictions of the ground situation from independent data inputs and model results.

Contemporary Techniques for Flood Risk Assessments

Overview

Flood risk assessment is the estimation of the risk of future water discharges that cause damage (Arduino et al., 2005; Hlacova et al., 2005; SIWRP, 2006). It commonly uses local and regional river gauging station ("hydrometric station") data covering the longest possible periods-of-record, and statistical flood frequency analysis, coupled with techniques to extrapolate or interpolate the results to the land parcels of interest. Such work may provide, for example, an estimated "100 year discharge" (flow with a probability of occurrence in any given year of .01 or 1%) for a stream or river valley at a particular location. Then, given this discharge, and: adequate characterization of a) the channel cross-sectional geometry or bathymetry, b) the channel and floodplain slope, and c) the "Manning's n" roughness (resistance to flow) values associated with the channel and the floodplain (Arcement and Schneider, 1989; Komuscu et al., 1998), *flow hydraulic modeling techniques* such as the step-backwater method (Dingman, 1994) are used to calculate flood height (hereafter referred to as flood stage). In turn, comparison of stage to local topography provides a map of land parcels under and above this flood level, so inside and outside the "100 year" floodplain.

The quality of the resulting flood hazard map depends heavily on the necessary input data, and, for the latter steps, can vary widely depending on how well characterized floodplain topography is. Also, depending on the type of flood, the "connectivity" of local depressions along a floodplain landscape affects flow routing and actual flooding (Heiler et al., 1995). For floods occurring through bank over-topping of the local river, parcels below the flood stage may not be inundated unless there is a connection to the water source; for example, levee systems may provide local protection to such low-lying land. However, some floods occur through saturation of floodplain soils, so from direct precipitation onto waterlogged soils and the resulting emergence above ground level of the local water table (Mertes, 1997; Mertes, 1990; Mertes et al., 1995). Such occur, for example, repeatedly along the Red River of North Dakota, USA and also in some low-lying monsoonal areas of Asia. In these cases, levee systems and

hydraulic connectivity become less important, and the land elevation is the critical factor. For either type of flood, the level of detail (expressed as spatial resolution (in m, or as a root mean square or rms value) in the characterization of local topography strongly affects the spatial resolution, accuracy and precision of the resulting flood hazard map (Figure 1).

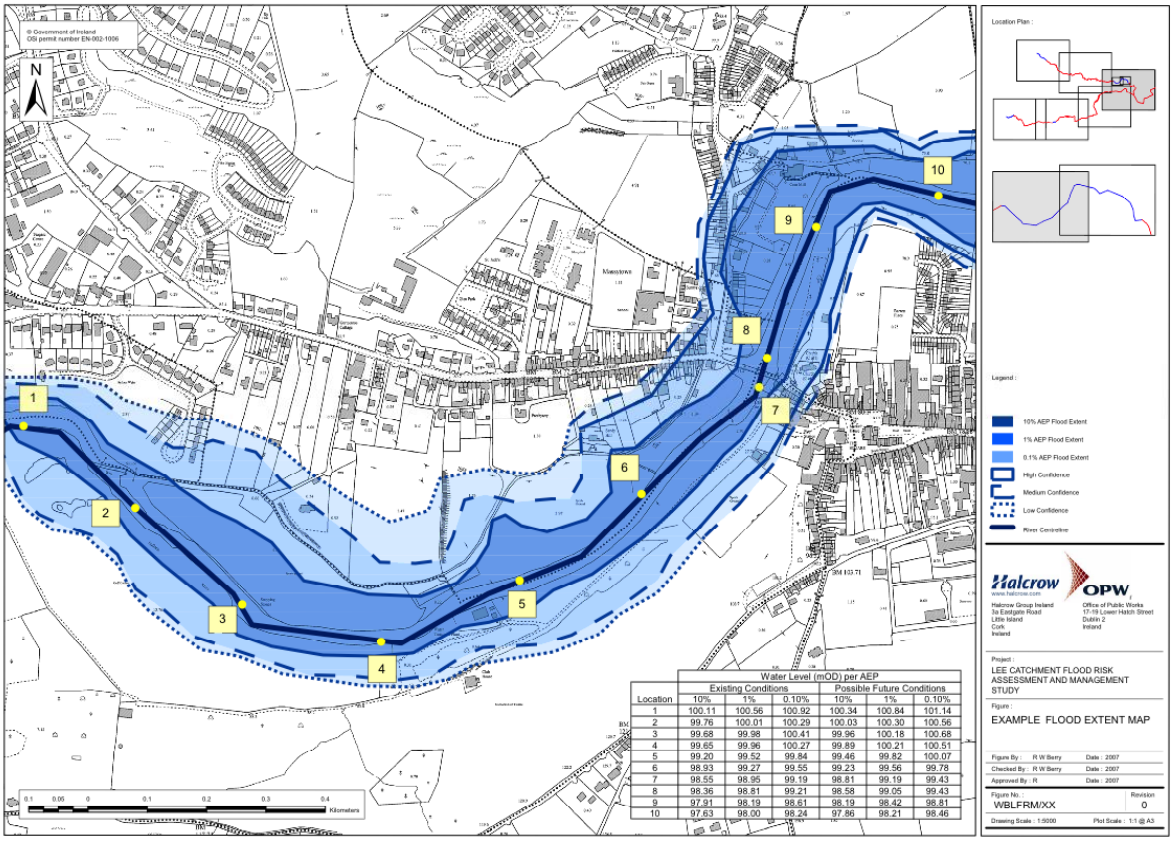

Figure 1. Flood Risk Map for a river in County Cork, Ireland (Halcrow-Group-Ireland-Ltd, 2007). The .1%, 1%, and 10% AEP (annual exceedance probability) zones are shown in light blue, medium blue, and dark blue, respectively, and the solid, dashed, and dotted lines illustrated decreasing (high, medium and low) degrees of confidence in the boundaries.

Hydrologists are currently engaged in improvements in both areas (flood discharge and flood inundation) of flood risk assessment. For example, by use of watershed modeling, antecedent soil moisture, and time-series of extreme rainfall, flood events can be modeled or synthesized and their return periods estimated (Hlacova et al., 2005). Also, increasingly, new-technology methods of acquiring the needed topographic data are being emphasized: because flood risk maps are so dependent on topographic vertical and horizontal accuracy and coverage (Sanders et al., 2005). Laser light detection and ranging (LIDAR), commonly from airborne platforms, has emerged as a effective method of acquiring the high-vertical-precision topography needed (French, 2003). Finally, wide spread availability of DTM data and GIS software permit, for many regions, the automation of the time-consuming tasks associated with flood-prone area delineation. The analytical capabilities of the GIS significantly speed the calculation of the flood discharge information and ultimately flood-prone area delineation (Beckman, 1976). In one example, from Nebraska, U.S., an interactive process used GIS modules, integrated with watershed and river modeling software, to develop flood-prone area maps. The methodology extracted critical hydrologic information from digital elevation data. Then, discharges were calculated at user-specified locations using regional regression equations. Flood depths were calculated in watershed modeling

software using these discharges. The flood depths were converted to a digital flood surface, which was compared to the DTM data to determine the flood-prone areas (Beckman, 1976). The process allows for rapid and efficient, limited-detail floodplain mapping over large rural areas.

For agricultural insurance purposes, it must be noted that floodplains have long been preferred locations for many forms of agriculture. Whereas, in developed nations, there is a focus on reducing losses to residential and commercial locations that are located within "the 100 yr floodplain", in the developing nations, even low-lying lands that are flooded every 5-10 years may be intensively farmed. Thus, the frequency of significant crop losses from flooding is correspondingly high, and the concern of insurers must be on these more frequently flooded lands. Better knowledge is needed, for example, concerning which lands are flooded, on the average, more often than once every 10 years, and which floodplain lands are less frequently flooded than this.

Wide-Area Flood Risk Mapping

Flood risk mapping procedures must be both standardized (if they are to be employed equitably over large areas) and scientifically responsible. Within the U.S., Congress established the National Flood Insurance Program with the passage of the National Flood Insurance Act of 1968. The NFIP was to provide reduced vulnerability to flood damage and a flood insurance safety net for individuals. Flood insurance was not generally available though the commercial markets, and NFIP enabled property owners to purchase insurance against flood losses, if their community agreed to participate in the program. Such insurance shifts risk from federal taxpayers to those whose properties are at risk, and extension of the insurance brings with it certain obligations on the participating communities regarding measures to reduce exposure to flood losses.

The 1968 Act authorized the Federal Government to "identify and publish information with respect to all floodplain areas, including coastal areas located in the United States" that have flood-prone areas, and then to "establish or update flood-risk zone data in all such areas and to make estimates with respect to the rates of probable flood-caused loss for the various flood risk zones for each of these areas". More recently, though the Flood Map Modernization Program and its partners, the Federal Emergency Management Agency (FEMA) provides updated flood hazard data and maps for the United States to support NFIP (http://www.fema.gov/business/nfip/).

Within the U.S., it is widely recognized that flood hazard conditions are dynamic, and that existing, decades-old NFIP maps may not reflect recent development and/or natural changes in the environment. The ongoing updating of NFIP maps takes advantage of revised data and improved technologies for identifying flood hazards. The assessment of risk usually requires solution of a flood routing problem as a part of the assessment. Simplified numerical flow models are used for the computation of flooded areas, as more sophisticated models are often too complex to manage or are not well suited for the specific needs of flood routing problems. However, models that are presently accepted by FEMA for NFIP usage are: CHAMP, version 1.0; MIKE 21; DYNLET; HEC-RAS 3.0; WSPGW (a Windows version of WSPG), AHYMO 97; Colorado Urban Hydrograph Procedure; HCSWMM; and SHEET2D.

Fundamental to modeling flood flows is estimation of the size of flood flows, such as those having an estimated 0.2% chance of being exceeded in any given year, (the "500-year" flood; commonly used in flood insurance studies where detailed basis exists for maps of the 1% annual exceedance, "100 yr" flood). Or, instead may be estimated the "probable maximum flood" (PMF, based on assumption of the most severe hydrological and meteorological conditions at a site and using the Probable Maximum Precipitation reports provided by the U.S. National Weather Service), for applications such as dam design. Another flood size is the "Standard Project Flood" (SPF, used by the U.S. Army Corps of Engineers). The PMF and SPF do not have any associated probability of exceedance associated with them. Also, as noted, there are two distinct tasks: 1) estimating the size and, in some cases, frequency of

the flood flows, and 2) determining the inundation depth and map extent to be associated with such flows. For agricultural insurance purposes, there is also an evident need to incorporate flood duration into such probability estimates, so that land areas that experience long duration of flooding can be differentiated from those where the flood wave passes quickly and drying occurs more rapidly.

In regard to estimating flood discharge, the U.S. and many other nations have developed standard techniques or handbooks so that flood size and frequency are estimated in a uniform ("accountable") manner, and even though standardization alone does not accomplish the also-desired goal of accuracy and reliability. Within the U.S., the US Geological Survey (USGS) developed regional regression equations to estimate the flood frequency and magnitude at ungauged locations of a watershed. These equations are based on flood frequency and magnitude from gauged watersheds and on a standard probability distribution (the Log Pearson Type III). Regression equations transfer flood characteristics from gauged sites to ungauged sites through the use of topographic, physical, and climatic characteristics of the ungauged watershed. See also (Reed et al., 1999; Wilshire, 1986) for discussion of regionalization and selection of regions. The USGS regression equations obtained up to September 30, 1993, are summarized in (USGS, 1993). The USGS also developed a National Flood Frequency (NFF) computer program that estimates the flood frequency and magnitude for ungauged sites by the application of the appropriate regional regression equations. NFF was first released in 1993 and subsequent revisions were made in order to incorporate updated data.

Because the majority of stream gage data used in developing the regression equations were collected from rural watersheds, the applicability of the regression equations is generally restricted to rural watersheds. Urban watersheds exhibit different flow characteristics. Therefore, regression equations for urban watersheds have been developed for some areas, and include parameters such as the percentage of impervious areas and urban development factors. Also, the USGS regional regression equations are not appropriate for estimating flood magnitude and frequency in watersheds subjected to flow regulation, or to heavily mined areas or karst areas (limestone terrain with abundant sinkholes, caves and caverns) where excessive runoff is diverted into or outside the surface water basin. Finally, due to the relatively limited number of years of stream gage data availability, large estimation errors are, in general, inherent in the peak-flow discharges estimated using USGS regional regression equations.

Hydrological risk zone mapping such as the U.S. national program addresses, among other societal needs, the requirement for flood risk assessment in setting insurance prices. Risk zone mapping produces a set of maps and quantitative, standardized, legally defensible interpretations of flood hazard zone delineations. In developed insurance sectors such as the U.S., these are flood insurance rate maps (FIRMs). Note that the basic data input is detailed topography and map information concerning the local drainage network (streams and rivers). In principle, hydrological risk zone mapping also requires developing numerical models that dynamically describe hydraulic characteristics (i.e. water level, flow, velocity, etc) for a defined topographical region. These models incorporate historic and current meteorological, hydrological, and hydraulic data, as well as relevant information about natural and man-made physical features including the location and characteristics of flood control works. When the environment in the defined region changes either by natural or human causes, the hydrological risk maps must be revised and updated. Consequently, the underlying numerical models should be capable of incorporating and simulating the effect of changes to a number of variables over defined time periods. Ideally, the results of the risk zone mapping for each study area would also be validated by some independent means (such as by comparison to aerial or satellite imagery of known events). This is because of the large errors, as noted above, in assigning flood risk within many land areas. In practice, however, preparation of U.S. FIRMs has not normally been accompanied by consistent plans for future updating on a regular schedule, nor are such maps validated by mapping actual flood extents. The lack of validation and updating activities is due in large part to difficult technical and budgetary constraints: the models used are computationally demanding and data-intensive, and the cost of tracking watershed and waterway changes on a continuing basis is prohibitive if information is needed over large regions.

The search for more effective and economical methods of assessing flood hazard in developing nations is motivated by these difficulties in applying the traditional approaches. There is also a pressing need to identify lands flooded more frequently than every century. Although watershed land use or river channel changes may affect the size of the 100 yr event to some degree, their most powerful effect is on more frequent flooding. In this regard, traditional flood risk assessment uses the past as a guide to predicting the future: it assumes "stationarity" in the frequency distribution of peak flows over time. The importance of this assumption merits further discussion, and its general lack of validity suggests that alternative methods of risk mapping should be considered.

Traditional Risk Assessment and the Assumption of Stationarity

Statistical analysis of stream flow time series for the purpose of flood risk assessment has long used the assumption of stationarity: that the sampled time interval is representative of a population of flood peaks from a homogenous population whose recurrence intervals are not changing systematically over time. However, floods along any given river are, very commonly, composed of events caused by different meteorological circumstances (Hirschboeck, 1988). Also, an abundant literature attests to the importance of long term changes in runoff hydrology and flood regime, and especially for upland watersheds of moderate size and with significant local relief (Arnold et al., 1982). For larger rivers, the effects of upstream land-use change enter into international relations. For example, flooding along the Mekong River in Southeast Asia causes extensive crop and other societal damage, raising the question as to what degree such flooding can be attributed to upstream, cross-border changes, such as deforestation in China. In fact, analyses of individual river flow series has often demonstrated that the assumption of stationarity is rarely fulfilled: many stream flow series exhibit long term trends, and including changes in the frequency and magnitude of floods (Chuan and Jujn, 2003; Guowei and Jingping, 1999). Some of these trends may be related to global warming or to other climate changes (Arnell, 1996; Bardossy and Caspary, 1990; Bronstert, 1995; Burn and Arnell, 1993; Few et al., 2004; Katz and Brown, 1992; Knox, 1985; Knox, 1993; Milly et al., 2002; Mitchell and Ericksen, 1992). Recent analyses using both precipitation data and modeling indicate that global precipitation has, in recent decades, increased, and will continue to increase (Wentz et al., 2007; Zhang et al., 2007), and this in turn may cause, at least in some regions, an increase in flooding (Betts et al., 2007). There is no question that floods have also caused increased fatalities and various types of economic losses since global record-keeping began in the 1960s (Merabtene and Yoshitana, 2005). The implication for flood risk assessment and insurance pricing is that application of standard statistical methodologies for determining flood frequency and magnitude do not provide a complete and accurate assessment of flood risk.

Because of the variety of causes for non-stationary and non-homogenous flood flow series, there are no standard handbooks for calculating actual flood risk at many locations and over large regions. At a minimum, however, methodologies for determining stationarity or non-stationarity in flow series should additionally be applied (Hamed and Rao, 1999). Risk assessment could also take into account the modeled future trends in climate as well as known trends in contributing watershed land use. The incorporation of historical data (for example, as a binomial censored sample) (Archer, 1999) can provide a longer time scale in some locations and thus further evaluate long term trends. In some reforesting watersheds, downstream flood risk is decreasing, whereas, in many watersheds subject to deforestation, rapid urbanization, agricultural development, or channel aggradation, flood risk is increasing. Upstream reservoir construction and other engineering works strongly affect downstream flow hydrology, and, in areas bordering high mountains, global warming-related glacier melting are today posing entirely new flood risks as alpine lakes expand (McDowell, 2002). Flood risk determinations based on national-standard methodologies for the statistical manipulation of river discharge data are, thus, only a first step towards reliable flood risk determinations. They could be inappropriate for regions in some developing nations where the needed long term instrumental records and channel geometry surveys are lacking.

Even within developed nations with abundant instrumental stream flow records, stationarity issues cause significant uncertainties. An illustrative U.S. example concerns the middle and lower Mississippi River,

wherein different flood risk assessments result from the application of flood stage versus flood discharge time series (Pinter and Heine, 2005; Pinter et al., 2001; Pinter et al., 2002a; Pinter et al., 2002b). According to Pinter's work, for the Missouri River, channelization during the past ~100 years has caused channel capacity losses. At measurement stations spanning >1000 km from the lower Missouri to the middle Mississippi rivers, increases of up to 3-4 m (in flood stage, for the same discharge) have been linked to the construction of navigational engineering structures and levees. Different results thus occur if the same statistical techniques are applied to flood stages (which are most directly related to floodplain inundation extent) and the more-commonly used flood discharges (this latter method causes an incorrect, reduced, estimation of risk). In this case, even if the flood discharge time series does exhibit stationarity, the actual flood risk probability is changing. However, careful analysis of the flood series time series indicates that 20^{th} century climate change also invalidates stationarity of the flood series (Figure 2.)

Such issues affect most contemporary river systems. They become even more pronounced from the perspective of agricultural flood risk. As noted by (Hirschboeck, 1988), "Despite the elegance and pervasive use of the stationary stochastic model, when flood events are interpreted hydroclimatically, the validity of the stationarity assumption must be seriously questioned due to the history of variation of regional and global networks of changing meteorological features and circulation patterns". Hirschboeck stresses that floods arise from different meteorological circumstances, which themselves have different probability distributions that should be incorporated into risk assessment. The author considered three alternative non-stationary flood series models, wherein the statistical properties of the random variable $X(t)$ differ from one realization of $X(t)$ in time to another. These are: a) the time-varying mean model, b) the time-varying variance model and c) the time-varying mean and variance model. Thus, consider a flood time series with the largest flood (X_n) as the most recent event and intermediate floods $X_{1\text{-}4}$; X_2 being the smallest (Figure 3). Under a stationary model, the recent event is interpreted as quite rare because of its upper tail location in the pre-flood probability distribution (Kiesiel, 1969). Under the time-varying model, however, the event is now interpreted as having a high likelihood of being equaled or exceeded, given the new position of the theoretical distribution at time t_n. In the time-varying variance model, the large X_n and small X_2 events are no longer located in the extremes of the upper and lower tails of their respective populations as they both were in the stationary distribution. Finally, in the time-varying mean and variance distribution, the large X_n and small X_2 events both lie close to the means of their respective populations, and X_4 now is an extreme in the lower tail of its theoretical distribution. The resulting combined flood series and distribution resembles the typical positively skewed flood frequency distribution exhibited by many arid, semi-arid, and humid streams, but it is not a single, stationary, distribution (Figure 3). Hirschboeck's review concludes that: "A shift in general atmospheric circulation patterns or the anomalous persistence of certain patterns will be reflected in flood series by a shift to a different theoretical distribution for the random variable X_n in the series" (Hirschboeck, 1988).

Also, as noted by students of flooding in New South Wales, Australia: "evidence that the flood probability model is climate dependent for the case study region is strong. This has implications for flood risk assessment requiring *inter alia* the need to distinguish between short- and long-term flood risks. In the presence of long-term climate persistence, traditional flood frequency analysis can at best only provide estimates of long-term or unconditional flood risk. The estimation of short-term flood risks" (that pertaining to the immediate near future)…"will require improved mechanistic understanding of multidecadal climate variability and the development of stochastic models that explicitly recognize such secular variations" (Franks and Kuczera, 2002). In this case, the researchers acknowledge that traditional techniques, in which long term records are heavily emphasized, can lead risk analysis astray, if what is being sought is information about flood probabilities during the immediate coming years and decades.

These findings constitute a strong caution against simplistic applications of stationary, stochastic flood probability distributions to agricultural lands in developing nations. In many of these nations, contributing watershed changes are known to be dramatic, the frequency and magnitude of relatively frequent flooding are of most interest, and there are likely to be *El Nino*/*La Nina*, other inter-annual, inter-decadal, and

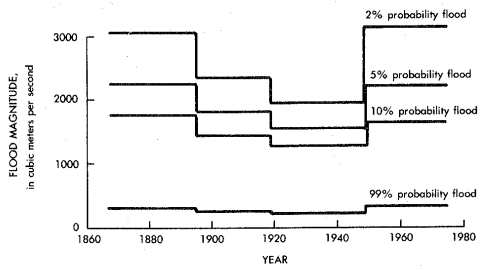

FIGURE 10. Affect of decadal-scale circulation episodes on the partial duration flood series of the Mississippi River at St. Paul. Separate estimates of flood probability were computed for different sections of the record using the standard log-Pearson Type III method. The boundaries defining the subperiods are not arbitrary, but have a distinct physical basis because they represent significant dates of change in prevailing global circulation patterns. Meridional circulation patterns were more frequent before about 1895 and since 1950, but zonal circulation patterns were more common between 1895 and 1950 (Source: Knox, 1983).

Figure 2. Illustration of non-stationarity of flood time series for the Mississippi River, U.S., showing large changes in the magnitude of low-frequency flooding. There is no evidence that this river represents a special case.

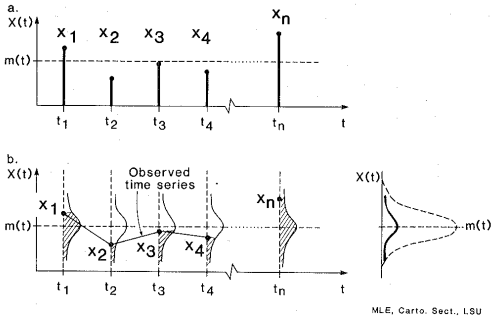

FIGURE 13. The standard stationary stochastic process model for a flood series. (*a*) Generalized version of an observed flood series. (*b*) Conceptual representation of the stationary stochastic process with time invariant mean and variance (modified from Kisiel, 1969a).

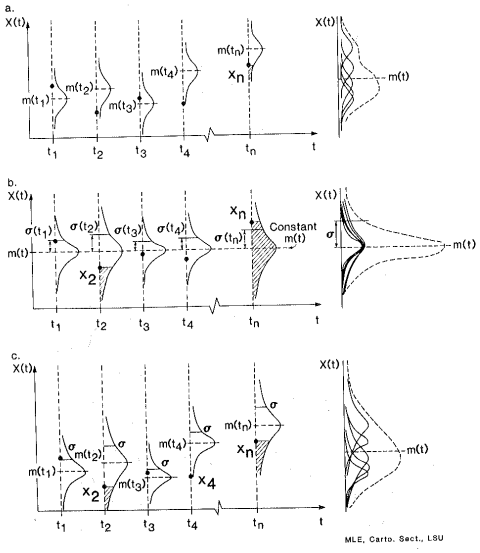

FIGURE 14. Alternative nonstationary stochastic process models for a flood series. (*a*) Time-varying mean. (*b*) Time-varying variance. (*c*) Time-varying mean and variance. The composite distribution at the right of each time series represents the theoretical distribution for the complete flood series. Although the distributions at each *t* are depicted as normal, skewed distributions could also be substituted into the model (modified from Kisiel, 1969a).

Figure 3. The plots on the left illustrate a series of annual flood peaks (X_1-X_n) and the assumption of a stationary mean and variance; the plots on the right show process models which accommodate time varying mean, time varying variance, and time varying mean and variance. From Hirschboeck (1988).

greenhouse warming-related changes and trends. In this context, the utility of the spatially extensive data provided by orbital remote sensing is now examined. It provides a time perspective extending only to recent decades, but benefits from unbiased and complete geographic coverage, and what is observed and measured (inundation extent, rather than discharge) is directly relevant to risk zone mapping.

Remote Sensing Resources for Flood Risk Mapping

Orbital remote sensing technology provides globally consistent geographic coverage of flood inundation. Through this approach, flood hazard assessments can, in principle, be accomplished without ingesting and manipulating any meteorological or river discharge data. Instead, the direct observable is the history and location of actual flood inundation. Figures 4 and 5 show sample "rapid response" flood inundation maps.

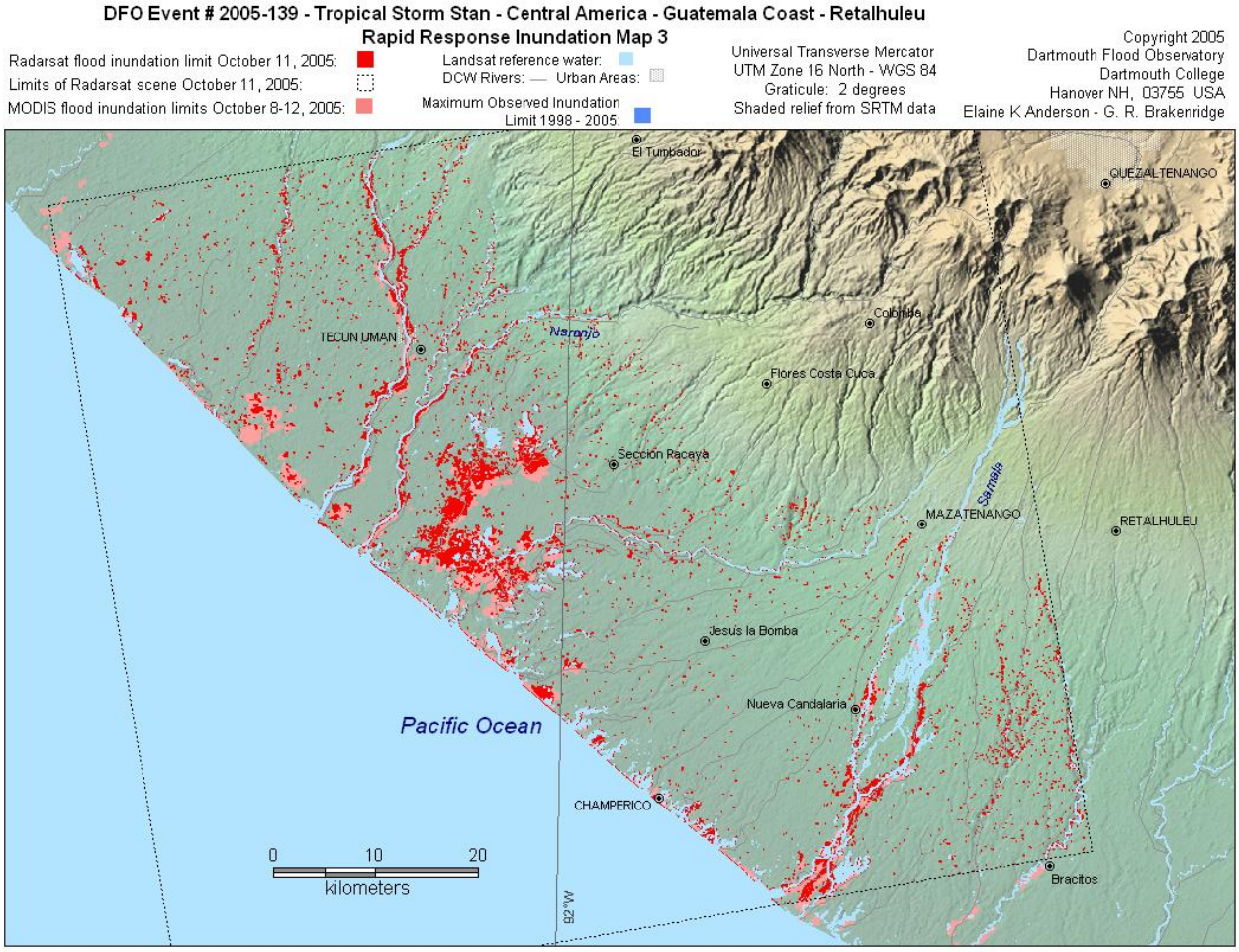

Figure 4. NASA MODIS- and RADARSAT-based flood inundation mapping for a hurricane event in Central America. Landsat data prior to the flood event provides a reference surface water data layer. The two MODIS sensors image this land area several times each day and provide for multiple time steps during flooding. Map is shown at much smaller than full spatial resolution.

Gauging station-based flood risk approaches, and the associated statistical and modeling infrastructure, all evolved before the advent of orbital remote sensing, and the possibility of routine mapping of flood events. In the absence of the latter, "flood modeling" is the only feasible approach for many regions, but, if remote sensing is available, developing an observational record may be more accurate and also more

cost-effective than modeling. Although realistic (but computationally intensive) modeling of floodplain inundation and drying can be locally accomplished (Bates and Anderson, 1996; Bates et al., 1992; Bates et al., 1995; Bates and De Roo, 2000; Bates et al., 1997; Bates et al., 2002), such work further

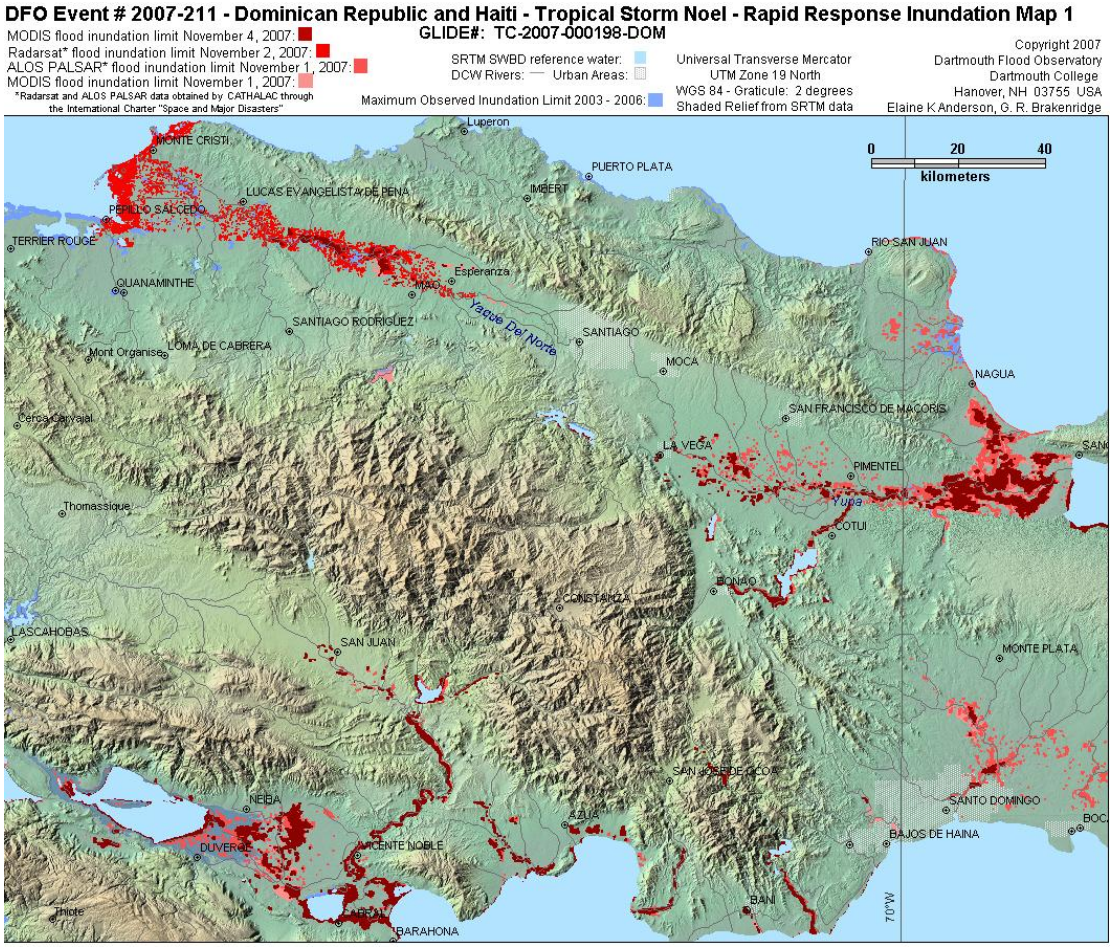

Figure 5. NASA MODIS-based flood inundation mapping for a tropical storm affecting the Dominican Republic. Reference water is derived from the NASA SRTM data. The two MODIS sensors image this land area several times each day. Map is shown at much smaller than full spatial resolution.

demonstrates the importance of factors other than discharge in affecting inundation patterns and duration (for example, antecedent conditions such as floodplain soil moisture are important). Depending on such conditions, similar flood hydrographs may cause varying inundation durations. The intensive effort thus invested in predicting the size of flood discharges, as described above, thus does not translate directly into accurate inundation prediction. Meanwhile, orbital remote sensing provides direct observation of the time series of exactly the phenomenon that otherwise must be modeled as a function of many variables. Remote sensing can delineate those land areas where flooding *is in fact* a contemporary hazard, rather than where extrapolated and interpolated discharge data, channel bathymetry, channel slope, hydraulic theory, topographic data, and modeling indicate where flooding *could* occur. An entirely different approach in flood risk assessment is thus possible, given the new technologies.

Although the usefulness of remote sensing has been recognized and described by many workers, the transfer of this capability into risk mapping has been slow to occur. This may be due mainly to sensor data acquisition and distribution policies, which have previously made relevant data difficult or expensive to obtain. Orbital remote sensing was first used to map inland river and coastal flooding commencing in the early 1970s with the advent of the ERTS and then Landsat satellites. Also used for flood remote sensing have been the Advanced Very High Resolution Radiometer (AVHRR), the synthetic aperture radar (SAR) satellites (ERS-1, ERS-2, Radarsat, JERS-1, and Envisat), the French SPOT satellites, and the two MODIS sensors aboard NASA's Terra and Aqua satellites (Ali et al., 2001; Barton and Bathpls, 1989; Blasco et al., 1992; Blasco et al., 1989; Brakenridge and Anderson, 2005; Brakenridge et al., 2002; Byrne et al., 1981; Deutsch and Ruggles, 1974; Gumley and King, 1995; Hess et al., 1990; Islam and Sado, 2000; Islam and Sadu, 2000a; Islam and Sadu, 2000b; Liu and Liu, 2002; McGinnis and Rango, 1975; Miller and Osterkamp, 1978; Moore and North, 1974; Nico et al., 2000; Okimoto et al., 1998; Profeiti and MacIntosh, 1997; Quan et al., 2003; Rango and Salomonson, 1974a; Rango and Salomonson, 1974b; Rasid and Pramanik, 1993; Robinove, 1978; Rosenqvist et al., 2002; Sheng et al., 1998; Simpson and Doutch, 1977; Wiesnet et al., 1974; Yamagata and Akiyama, 1988).

The NOAA AVHRR sensors, which provide ground resolution of only 1.1 km, were early on appreciated as flood mapping tools, although mainly large rivers were studied (Barton and Bathpls, 1989; Harris and Mason, 1989; Islam and Sado, 2000; Islam and Sadu, 2000a; Islam and Sadu, 2000b; Quan et al., 2003; Sheng et al., 1998). However, the record provided by these long-flying sensors dates back to the mid-1980s, and online archives are freely available to the public without charge: they contain valuable information about past large floods. Most other sensors are higher in spatial resolution but lower in temporal sampling: they provide snapshots of floods, close up, commonly at significant per-scene cost, and not always at the time of peak inundation. The significant exceptions are the two MODIS sensors, beginning in late 1999, which provide AVHRR-like wide area, very frequent, geographic coverage and at a much-improved spatial resolution of 250 m. The MODIS sensors also include better geolocation information and calibration procedures; both facilitate accurate water/land discrimination and mapping.

Three factors have constrained the widespread adoption of orbital remote sensing in general to flood risk mapping: 1) cost of individual satellite scene acquisition, 2) long time intervals between revisits by the sensor to particular locations, and 3) lack of continuous monitoring capability over the needed years of time. Note again that, although the AVHRR sensors are not so constrained, their relatively low spatial resolution prohibits effective mapping of many floods where areal extents are relatively small. Unfortunately, revisit time intervals for high spatial resolution sensor data are commonly measured in days to weeks, whereas near-daily observations are needed to measure flood events, capture peak inundations, and establish flooding duration. In short, prior to MODIS, appropriate sensor data were simply lacking. Also, data costs are clearly an issue: per-scene costs must be very low, in order that the needed temporal sampling (near-daily, at least during flood season) be feasible. River discharge varies dramatically, sometimes through several orders of magnitude, over time periods of only a few days (Figure 6): an incorrectly timed image will not measure peak inundation.

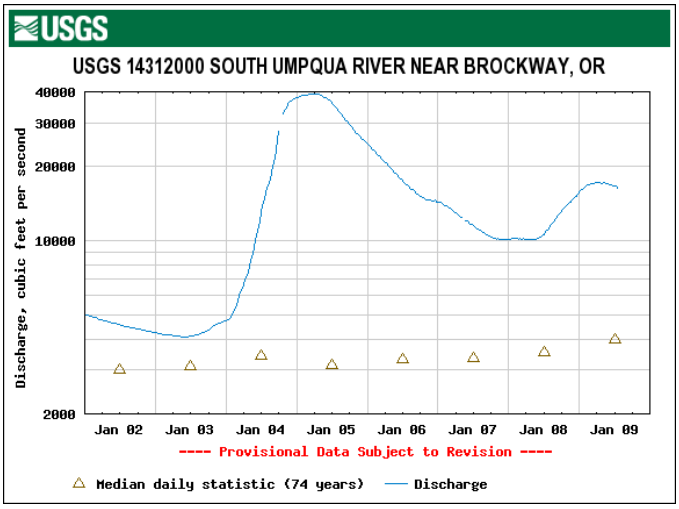

Figure 6. Gauging station-based flood hydrograph for a western U.S. river, showing variability of river discharge over daily time intervals. Discharge changed by an order of magnitude in less than one day and peak discharge, in this case, lasted only a few hours. Larger rivers in lower gradient terrains exhibit somewhat slower rises to maximum and subsequent declines.

Because of these constraints, remote sensing has previously been employed in a relatively *ad hoc* manner: as a response to very large flood events that require disaster assistance and persist long enough for the high spatial resolution sensors to be employed. Prior to the creation of the Dartmouth Flood Observatory digital "World Atlas of Flooded Lands", Figure 7, there was also no clearing house to store the inundation results of such case-specific studies: satellite images were used for news stories, or to guide relief efforts, or to demonstrate satellite capabilities, but the data and inundation outlines were not stored anywhere in an organized archive and in order to preserve these records of recent flooding. The World Atlas of Flooded Lands is an pilot attempt to address this need (http://www.dartmouth.edu/~floods/Atlas.html), and the Observatory is now partnered with several other organizations who ingest its data into their own archives (for example, the Pacific Disaster Center, http://www.pdc.org).

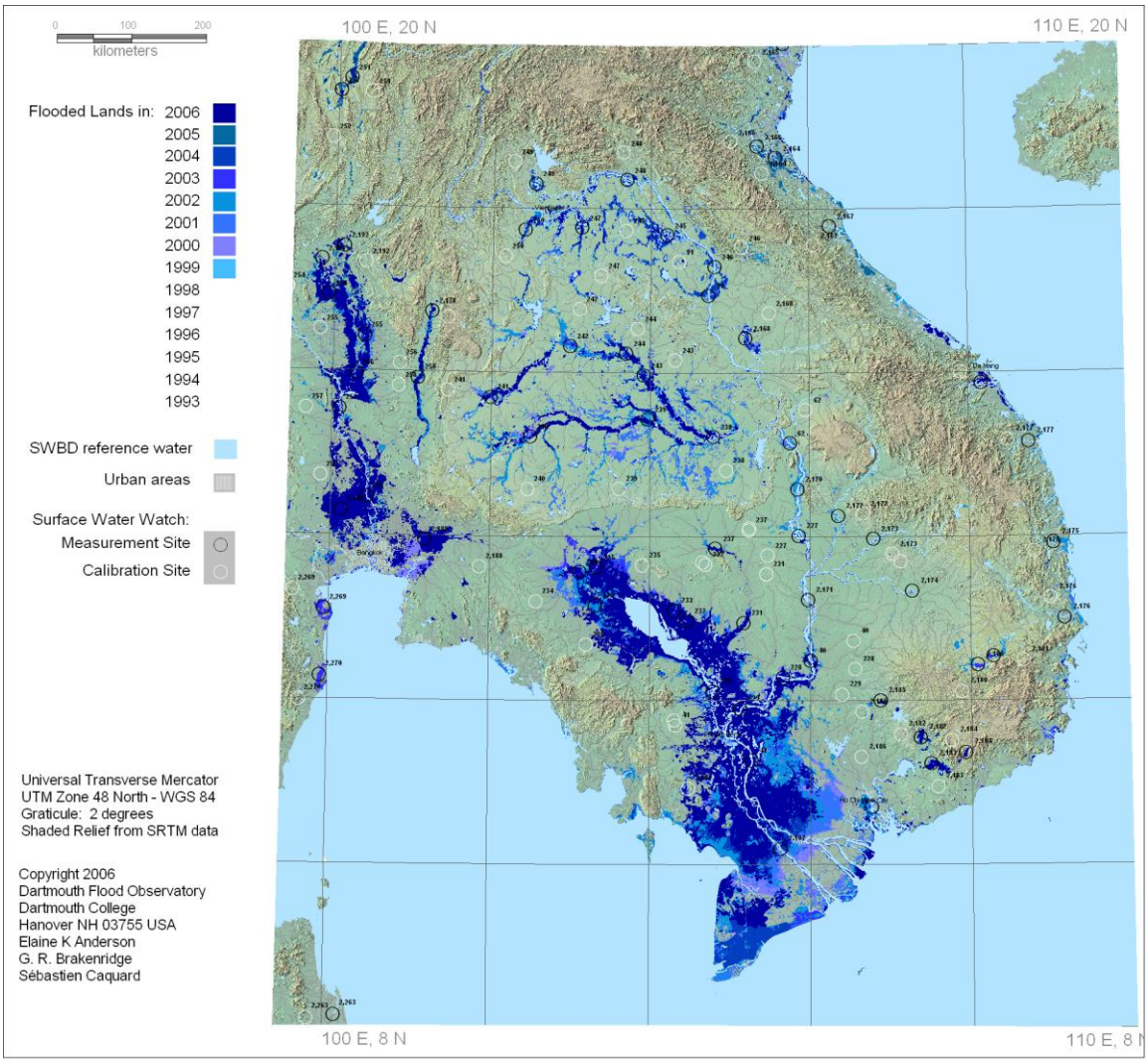

Figure 7. Sample tile from the Dartmouth Flood Observatory digital "World Atlas of Flooded Lands", at much reduced scale, showing lands flooded during the years 1999-2006. Also illustrated are satellite river gaging sites, which are part of the Observatory's "RiverWatch" system.

Imaging the areal extent of flooding during one particular large magnitude/low frequency event, although clearly valuable for identifying flood-prone land, does not itself offer any information about probability of recurrence: was the imaged event an unusual rate event, or one that occurs every 10 years, on the average? In most cases, remote sensing based flood mapping studies have failed to address this last,

critical, issue. With the advent of the two NASA MODIS sensors (the first was launched in late 1999), and their associated data distribution system, flood remote sensing capabilities dramatically changed. MODIS combines the wide area, frequent revisit, free data characteristics of the AVHRR sensors with spatial resolution at 250 m (so 16 MODIS pixels per 1 AVHRR pixel). This is adequate for mapping, and monitoring through time, floods along most medium to large rivers. The geocoding information provided with each MODIS image facilitates automated re-sampling and image rectification to any standard map projection and with a rms (root mean square error) in geographic position of +/- 50 m. As illustrated in Figures 2 and 3, for the first time, floods can be tracked economically, in map view, and on a near-daily basis, and the record of such flooding can be preserved for incorporation into wide area flood risk assessments. This relatively new capability will be maintained in the post-MODIS era with the planned follow-on NASA/NOAA VIIRS sensors, which also will replace the present AVHRR constellation. There are important implications, discussed in the next section, for both wide-area flood risk assessments, and for developing flood indices for index-based parameter insurance strategies.

Table 1 lists satellite sensors and data that may potentially be applied to either flood risk assessment (in which case, archived data of previous floods are of value) or to mapping and measuring contemporary floods (as part of indexed insurance programs). The table illustrates the variety of data sources available. In detail, retrieving archival image data is itself a complex task: as shown in the table, many nations have now flown Earth imaging satellites, and data availability from such sensors ranges from non-existent, to available at significant expense per scene through commercial providers (SPOT Image, Inc, Eurimage, Radarsat International, and others) to freely available, at no cost, to an international public via ftp or other internet services (NASA Terra and Aqua MODIS data, NOAA AVHRR). Any such list is outdated soon after being compiled, as new sensors are now being launched on an almost weekly basis.

The short-term challenge for flood risk mapping and for development of flood indices is selection of the most appropriate and economical data. However, where the need is sufficiently strong and persistent, the longer-term challenge is for end users to collaborate with sensor and data distribution engineers in order to customize available technology to fully address their data requirements. For example, Surry Satellite Technology, Ltd, has worked with a number of developing nations to provide a dedicated, small satellite-based, national disaster response capabilities, and several U.S. companies as well could provide similar mission focused and relatively economical satellite design and data retrieval systems.

Landsat-1 / ERTS-1 (ERTS-A)	23-Jul-72
Landsat-2 / ERTS-2 (ERTS-B)	22-Jan-75
Landsat-3 (Landsat-C / ERTS-C)	05-Mar-78
Landsat-4 (Landsat-D)	16-Jul-82
Landsat-5 (Landsat-D1)	01-Mar-84
	15-Apr-99
Landsat-7	
French Satellite Probatoire de l'Observation de la Terre (SPOT) series:	
SPOT-1 (SPOT-A)	22-Feb-86
SPOT-2 (SPOT-B)	21-Jan-90
SPOT-3	26-Sep-93
SPOT-4	24-Mar-98
SPOT-5	03-May-02
Indian Remote Sensing (IRS) satellites:	
IRS-1A	17-Mar-88
IRS-1B	29-Aug-91
IRS-P2	15-Oct-94
IRS-1C	28-Dec-95

IRS-P3	21-Mar-96
IRS-1D	29-Sep-97
IRS-P4 / Oceansat-1	26-May-99
IRS-P6 / ResourceSat-1	17-Oct-03
IRS-P5	tbd
IRS-P7 / Oceansat-2	tbd
Canadian/U.S. radar satellite:	
Radarsat-1	tbd
Canadian Radar satellite	
Radarsat-2	tbd
European Remote Sensing (ERS) satellites:	
ERS-1	17-Jul-91
ERS-2	20-Apr-95
Envisat	tbd
Japanese Remote Sensing satellites	
JERS-1	tbd
ALOS/Daichi	tbd
U.S. Earth Observation System (EOS) satellites:	
EO-3	tbd
EOS-AM1 / Terra (includes MODIS and ASTER)	18-Dec-99
EOS-PM1 / Aqua (includes MODIS)	04-May-02
China (PRC) Brazil Earth Resources Satellite (CBERS) / ZY-1 series:	
ZY-1A / CBERS-1	14-Oct-99
ZY-1B / CBERS-2	21-Oct-03
ZY-1B2 / CBERS-2B	19-Sep-07
China (PRC) earth Resources Satellite (CRS) / ZY-2 series:	
CRS-1 / China Resource-1 / ZY-2A	01-Sep-00
CRS-2 / China Resource-2 / ZY-2B	27-Oct-02
CRS-3 / China Resource-3 / ZY-2C	06-Nov-04
Republic of China (Taiwan) Satellite (RocSat) series:	
Rocsat-1	27-Jan-99
Rocsat-2	20-May-04
Israeli Earth Resources Observation Satellite (EROS) series:	
EROS-1	05-Dec-00
EROS-2	25-Apr-06
EROS-C	tbd
Argentine Satellite de Aplicaciones Cientifico (SAC) series:	
SAC-A [Endeavour-launched]	04-Dec-98
SAC-B	04-Nov-96
SAC-C	21-Nov-00
German Space Agency/commercial satellites:	
TerraSAR-X	tbd
U.S. commercial satellites:	
Ikonos-2	24-Sep-99
QuickBird-2	18-Oct-01
OrbView-1	03-Apr-95
OrbView-2 / SeaStar / SeaWiFS	01-Aug-97
OrbView-3	26-Jun-03
WorldView-1	18-Sep-07

U.S. NOAA Polar Orbiters (AVHRR sensor):	
NOAA 12	
NOAA 14	
NOAA 15	**13-May-98**
NOAA 16	**21-Sep-00**
NOAA 17	**24-Jun-02**
ESA Polar Orbiting Weather Satellites:	
MeTop-A	19-Oct-06

Table 1. Satellites and sensors potentially available to measure past and present flood events. Optical satellites are shown in plain font; imaging radar satellites in italics; currently- operating (2007) satellites are highlighted in bold face.

Each sensor technology has advantages and disadvantages for mapping flood inundation, and in addition to those factors already described. Thus, sensors that operate in optical spectral regions suffer from data gaps caused by cloud cover and nightfall. Even, as the case with MODIS, when frequent overpasses allow maximum use of temporary clear weather, very sustained levels of cloud cover may constrain imaging a particular flood event. In contrast, the synthetic aperture radar (SAR) sensors return data both day and night, and through even heavy cloud cover (SAR sensors are in italics in the table). Their data costs remain significant, however, and wide area SAR sensors, in "always on" mode, as for the AVHRR and MODIS sensors, do not yet exist. Also, whereas optical wide area sensors, such as MODIS (1600 km swath widths) generally provide more frequent revisit frequency than narrow swath sensors such as ASTER (60 km swath widths); the temporal and spatial coverage advantage comes at the cost of spatial resolution (250 m versus 15 m). Depending on the terrain, 250 m may be too coarse for useful mapping of some floods, even though, coupled with other information, such data may be used to establish that insurance-triggering flooding has occurred.

New Strategies for Flood Risk Mapping and Determination of Flood Indices

Now are considered two different but inter-related needs: 1) objective assignment of land parcels and crops into flood risk zones, and 2) consistent and accountable determination, as floods occur, of local exceedance of flood index threshold values: such that reliable prediction can be made of crop losses. The present report identifies significant limits to the accuracy and precision of traditional, non-remote sensing, modeling-based approaches to the first need, especially when large geographic areas are to be included. The problems for flood risk mapping carry over as well to any precipitation- or river gauging station-based flood index for triggering insurance payments: there may be sufficient meteorological data to predict within certain limits what the flood discharge at-a-station will be, or a flood discharge may be known, but it remains a separate and challenging assignment to predict what lands will thereby be inundated. Implementation issues are compounded for the international scope of World Bank activities. A national water ministry may not have rapid access to local gauging station measurements. Also, even when available internally, such in-country information may not be accessible to a non-domestic institution attempting to assess flood damage. Can, instead, remote sensing approaches meet the needs for reliable information on what lands are at significant risk from flooding, in the future, and what lands are in fact being flooded, at present.

To answer these questions and also point ways toward an operational remote sensing-based methodology, the prototype global flood measurement and risk assessment system (*RiverWatch*) operating in pilot form at the Dartmouth Flood Observatory is now described. Within this system, there are three separate but inter-related tasks:

1. *flood detection and magnitude assessment;*

2. *rapid flood mapping;*
3. *integration of mapped floods into quantitative flood hazard assessment.*

As presently configured, the Dartmouth prototype system utilizes two remote sensing data sources: for flood detection and magnitude assessment, the 36.5 GHz microwave (cloud penetrating) frequency of the NASA/JAXA AMSR-E satellite aboard AQUA, and for rapid flood mapping, the two NASA MODIS optical sensors aboard TERRA and AQUA. Both data sources are freely available via public ftp sites, and provide global coverage on a bi-daily or better basis.

As regards flood detection and measurement, using the AMSR-E microwave frequency allows data retrieval independent of cloud cover. However, these data are at coarse spatial resolution: approximately 8 km. AMSR-E is therefore used to monitor rivers in a manner similar to that of traditional ground-based gauging stations. Instead of mapping floods, the AMSR-E portion of *RiverWatch* (Figures 8 and 9) provides the capability to detect floods as they are occurring along predetermined river reaches (measurement sites), and to thereby monitor flood location, duration and severity. With additional calibration provided by even widely scattered ground-based gauging stations, the remote sensing signal at the "satellite gauging sites" can also be transformed to discharge (Brakenridge et al., 2007a), and the signal can then be compared directly to inundation imaged and mapped by MODIS (Figures 10 and 11).

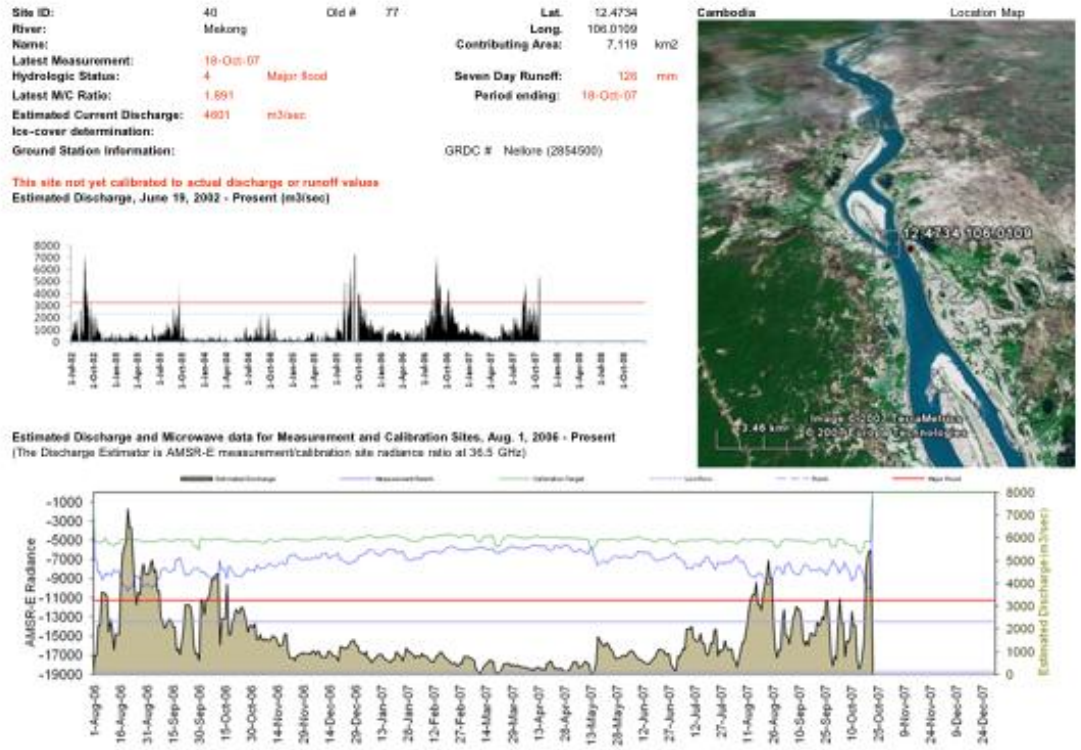

Figure 8. Sample satellite gauging site display for RiverWatch. The AMSR-E data has been transformed into estimated discharge. Flows above the red line, at this location, are identified as floods, and map displays (Figure 9) can show, each day, which sites have exceeded this threshold. See (Brakenridge et al., 2007a) for detailed discussion and other examples.

Figure 9. Sample map display of global-coverage AMSR-E-based river discharge data. Red and purple dots are gauging sites experiencing flooding. Suggested enhancements to such displays include increasing map scale, adding drainage and cultural features, and delineating floodplain lands.

These results can be elaborated by more accurately calibrating the remote sensing signal to discharge. Also, the AMSR-E period of record is now long enough to reliably estimate, using statistical assumptions such as the Log Pearson III distribution, the 10 yr recurrence interval flood, and the corresponding inundation in map view, at all of the monitored sites. With additional work, it will be possible to extend the records at each site (there are 2500+ sites now being measured) back into the mid-1980s using archived data from the DMSP/SSMI sensors. If accomplished, this would allow Log Pearson III- or other distribution-based estimation of the 50 yr events. Finally, there is also the opportunity to make any operational system more robust by incorporating other sources of similar (~ 36 GHz) data now available (e.g. from the NASA/JAXA TRMM satellite and follow-on sensors). Thus, the methodology does not depend on successful operation of any one sensor for its future utility.

For the second task, rapid flood mapping, the prototype system uses the 250 m (visible and near IR) bands of the two MODIS optical sensors (examples are in Figures 4 and 5 and also as a multi-year compilation in Figure 7). The steps needed to produce such maps are straightforward and require only modest computational and software resources. They are as follows: 1) determination of the general region of flooding, either from news reports or sensor measurements, 2) searching online archives, which provide browse images, to select scenes where cloud cover is not obscuring the flooding, 3) ftp acquisition of the selected scenes, 4) geocoding and rectification of the portion of the scenes which include flooded land, 5) digital classification algorithm processing of these rectified subscenes and binning of pixels into land and water categories, 6) GIS polygon fitting around the classified water areas, again using standard algorithms available in most remote sensing analysis programs, 7) validation of the outlined water areas by visual comparison to the unclassified image, and removal of cloud shadow areas mistakenly classified as water due to the similar spectral characteristics at these wavelengths, 8), lastly, integration of the final flood polygons into GIS workspaces that include other data layers, such as topography, cultural features, permanent water, and previously mapped floods: to produce map displays showing the flooded lands.

Due mainly to the vagaries of cloud cover, MODIS coverage of any particular flood event may be temporally dense, but irregular: imaging may be possible daily or twice daily for several days, and then several days may be obscured. However, where flooding occurs along a reach also monitored via AMSR-E, the RiverWatch system can accurately determine the timing and magnitude of the flood peak, and relate this discharge to the more-intermittent MODIS record of inundation. Figures 10 and 11 provide an example of combining in this synergistic manner these independent space-based data. With such information and displays as a guide, an analyst can: a) predict the map extent of ongoing inundation based on the incoming AMSR-E data, even without any new MODIS information, b) determine if particular flood thresholds have been reached, and c) assess the severity of the event in comparison to all other events observed since mid-2002, when the AMSR-E data stream began. Then, if MODIS mapping data are added, the RiverWatch system provides sensor validation, at 250 m spatial resolution, of the estimated flooding. Finally, as the new AMSR-E flood discharge information is incorporated into the annual flood peak time series, the system automatically re-estimates flood recurrence intervals using the Log Pearson III distribution (or other distribution of choice).

The issue of lack of stationarity of flood series, discussed in regard to gauging station flood series, also applies to RiverWatch data. However, the remote sensing-derived data record period is short and extends to the present: using such data favors acceptance of recent flood history as being indicative of the immediate future and because it is not mixed into a longer term record. For analyses of these data, it appears that, particularly for determining exceedance probabilities for relatively frequent flooding (recurrence intervals of ten to several tens of yr), the most defensible strategy is to assume stationary means and variance, and incorporate new flooding into the time series without adjustment. Each time a new flood of record occurs, this approach will cause an upward revision of flood magnitudes and flood risk along the affected river valleys. Alternatively, one could connect the remote sensing record with the regional, longer term, record provided by gauging stations, and/or use regionalization approaches, in the same manner as is common with *in situ* gauging station data.

In summary, given the availability of sustained, remote sensing-based mapping of actual flooding over nearly a decade of time, there are clear, immediate benefits for determining relatively frequent (recurrence interval ~ 10 yr) flood hazard. The compilation shown as part of the Flood Observatory's World Atlas in Figure 7 is a preliminary regional flood hazard map as well (some known floods are still to be mapped, and the limits of the mean annual flood are, for many map tiles, still poorly constrained). However, this digital Atlas at least shows clearly lands known to have been flooded during the past decade. In some cases, the mapped floods were considered rare events, and some may even have been the flood of record at long term gauging stations, but, in the absence of reason to assume stationarity, and in the presence of many reasons not to, it is the most conservative plan to include these lands as approximating the 10 yr floodplain.

With adequate topographic and bathymetric information, and hydraulic modeling, and by incorporating and comparing many RiverWatch flow series from within a region, there is also clear potential for definition of 100 yr recurrence or more, discharges and associated floodplain lands. In this regard, Figures 10 and 11 show how matching the MODIS and AMSR-E records provides direct connection of a (bi-daily to more-than-daily, depending on latitude) time series of estimated discharge to the more intermittently imaged inundation record.

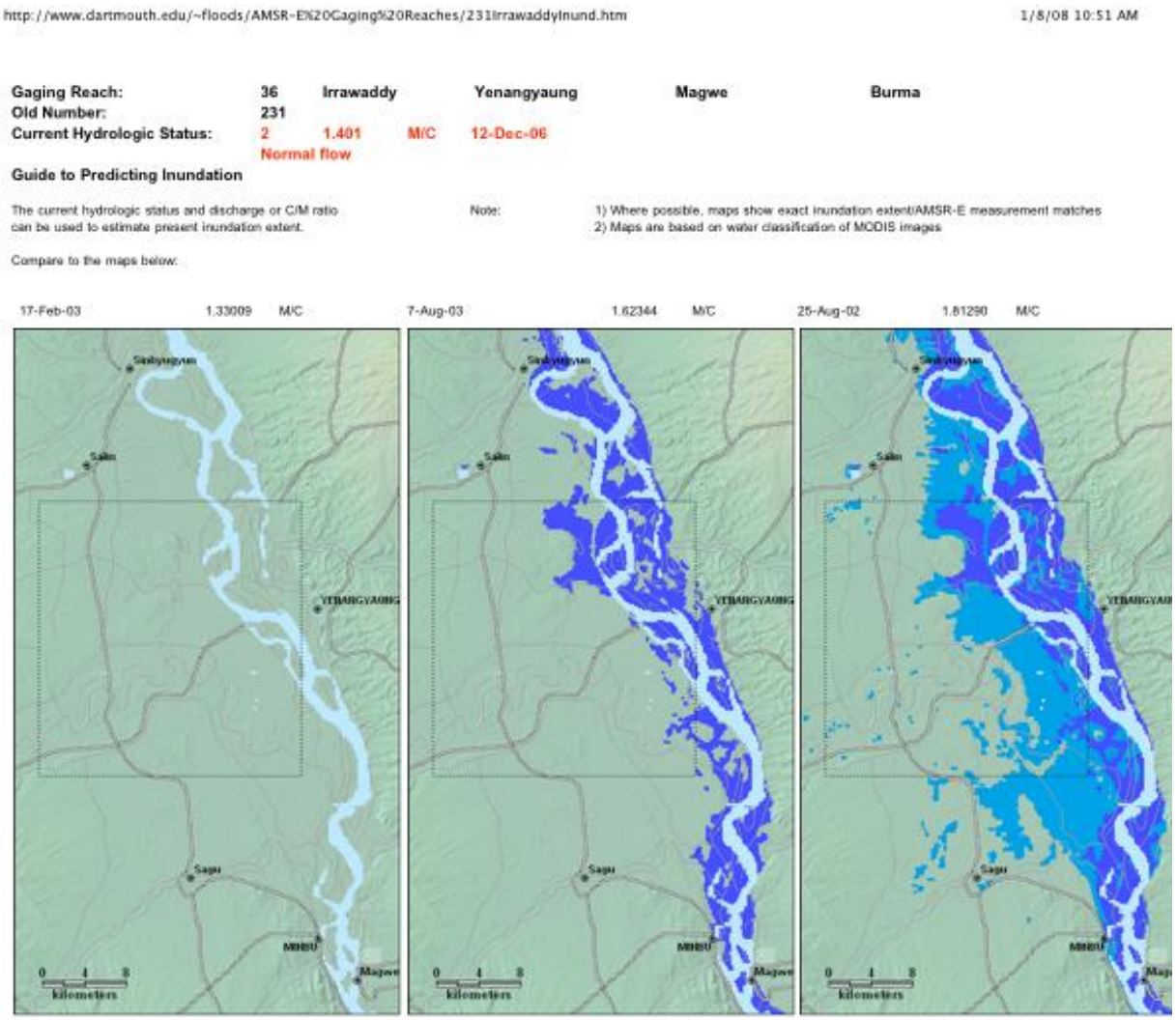

Figure 10. "Guide to predicting inundation" display from RiverWatch. The archived GIS data base of MODIS-imaged flooding along a ~50 km river reach is compared with AMSR-E data from the same location (gray line square shown on the maps). The "C/M ratio", varying between 1.33 and 1.81, is the AMSR-E discharge estimator, and it is a ratio of the measurement pixel microwave radiance to that of a nearby, dry land-only pixel. Newer data and displays for the same site now provide calibration to discharge of this same discharge estimator. The illustrated display shows the strong response of the discharge estimator to inundation, and the capability to predict ongoing flooding if its present value is known. The mapped inundation is here draped over a shaded relief map produced from the NASA SRTM global topographic data, which could also be used to model larger, more rare floods and floodplain lands. The Log Pearson III recurrence interval of each imaged and mapped flood can be calculated; the map shown on the right is close to the 10 yr or 10% annual exceedance probability floodplain.

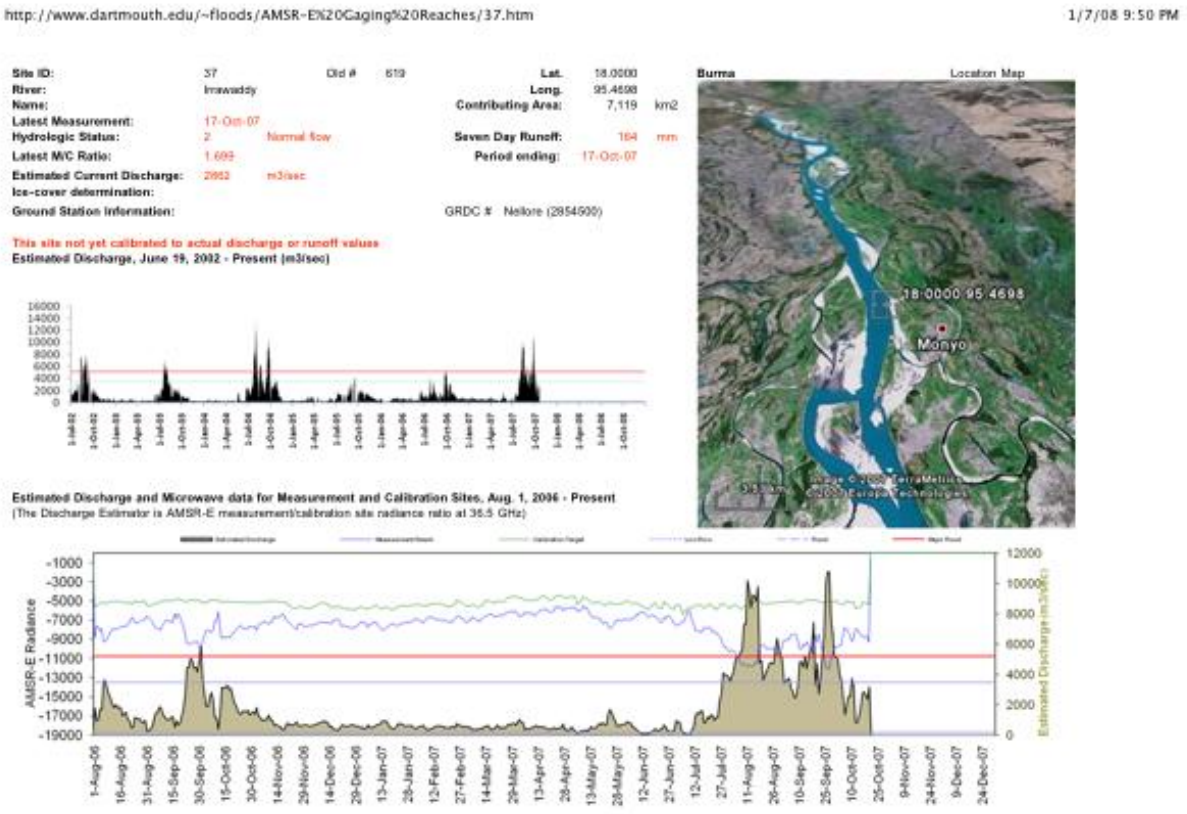

Figure 11. The AMSR-E estimated discharge for a river measurement site close to that shown in Figure 7. In this case, the C/M ratio was converted via a rough preliminary calibration equation to actual discharge, but the final calibration has not yet been accomplished. The red line threshold will be adjusted, after calibration to discharge and Log Pearson III-based analysis, to the 10 yr recurrence interval flood, and the blue line threshold to more frequent (r = 5 *yr) flooding. The lower plot is a detailed view of the more recent part of the complete record. Since preparation of this figure, the period of record has already lengthened to early 2008, and the system is posed to monitor flooding in the upcoming 2008 monsoon and tropical storm season. As new AMSR-E data arrive, the reach inundation extent can be predicted using the available MODIS-based inundation history, and as per Figure 10.*

The above examples illustrate how flood detection, near-real time flood mapping, and compilation of such maps, over time, all can be accomplished via remote sensing supported by available ground-station data and auxiliary data sets such as topography. The ~ 6 yr AMSR-E record allows for consistent estimation of the 10 yr, or 10% annual exceedance probability flood, on an automated basis, and as applicable to at least several tens of km upstream and downstream from the measurement site. As a general rule, the floodplain associated with this discharge will be approximated by the maximum inundation imaged by MODIS during this same period of record (in detail this depends on the actual distribution of flood peaks so far measured). As well, each MODIS inundation image can be matched to its coeval discharge value, and thus (not shown in the figures) to their precise flood recurrence probabilities. As the length of this observational record lengthens, the capability to estimate future flood risk for less frequent events improves: assuming an additional 4+ yr of record, to mid-2012, the 20 yr flood discharge will be constrained, as well as its inundation extent in map view. Such data can be combined with channel slope, cross sectional area, floodplain topography, and Manning's *n* roughness estimates, and standard hydraulic modeling techniques, to model inundation and verify *n* values: this provides for more reliable extrapolation to 100 yr or other low recurrence floodplain boundaries then would be possible without the

satellite data. Remote sensing thus offers a relatively efficient and direct path towards identifying both the flood risk of specific land parcels, and designing flood indices that signal when damage to crops have occurred.

Types of Flood Risk and the Design of Flood Damage Indices

Flood risk to agriculture is affected by: upstream dams, artificial levees, status of soil drainage improvements, conveyance status of the local channel (degrading or aggrading), trends in contributing-watershed land use that affect runoff, the topography of the watershed, and regional trends in climate that alter runoff frequencies and magnitudes. Trends in climate may cause non-stationary streamflow time series, and affect flood frequency, whereas drainage improvements to an agricultural field may reduce flood duration without any changes to flood peak discharges. Also, agriculture makes preferential use of level to gently sloping lands. Although essential crops may also occur along floodplain lands within narrow upland valleys, the aggregate of such land acreage, although locally important, is small compared to the extensive, humid to semi-arid plains where most global agriculture is practiced. The multiple factors affecting flood risk favor remote sensing approaches to assessing risk and monitoring damage. For example, and unlike the case for gauging station data, the protection of some land by dams or levees is directly recorded by remote sensing of those lands during regional flooding.

Flood damage indices for agricultural insurance purposes will likely include some method to estimate flood inundation extent, water depth, and flood duration, continuously across a floodplain: so that the flooded, or non-flooded status of particular land parcels can be determined, as well as the associated depths and durations. Other factors such as water sediment load and water velocity may also affect crop damage but are not discussed further here. Design of flood damage indices based on *in situ* gauging stations or on the AMSR-E data can incorporate detailed topography and the time series of remotely sensed peak flood inundation limits matched to their peak discharges. Crops vary with regard to sensitivity to shallow inundation, and their sensitivity also varies with number of days since planting: each agricultural parcel thus requires information concerning crop type and planting date, in order to assess damage from a particular input flood event and its depth and duration.

Extending index-based insurance approaches to diverse geographic regions will also require recognizing the varied causes of flooding, and their geographic and seasonal patterning. For floods cataloged during 1985-2002, the Dartmouth Flood Observatory (http://www.dartmouth.edu/~floods/) lists these categories of causation on a global basis: “heavy rain”, “brief torrential rain”, “tropical cyclone”, “monsoonal rain”, “snowmelt”, “Dam/levee break or release”, “ice jam/break-up”, “extra-tropical cyclone”, “tidal surge”, and “avalanche-related”. Figure 12 illustrates the number of cataloged events.

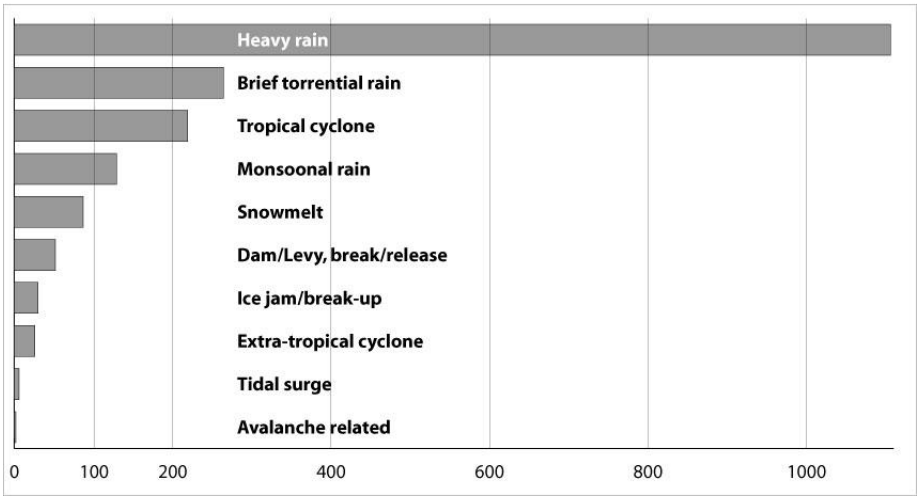

Figure 12. Global number of floods of various causation, 1985-2002. Data from the Dartmouth Flood Observatory Active Archive of Large Floods.

The geographic location of the cataloged floods has also been mapped, and as based on news and government reports (Figure 13). The observational coverage is not uniform: there is likely a bias towards reporting of floods in populated locations. Also, for some years, only an approximate geographic centroid of the area affected was gathered, whereas for most years, a polygon encloses the area reportedly affected by flooding (Figure 13). The polygons include, commonly, many rivers and streams and associated floodplain lands.

As floods have been tracked in this manner through time, a general global geographic picture has emerged, wherein some regions are, clearly, flood-prone and others much less so. Thus, from Figure 13: Flood-prone regions of the world clearly include: a) the eastern U.S., b) Central America and eastern Mexico, c) northwestern South America, part of Amazonia (although relatively infrequently), and mid-southern South America, d) central Europe and the U.K., e) an irregular belt of sub-Saharan Africa, the Sudan, and coastal southern Africa, d) Iran, Afghanistan, Turkey, and eastern India, f) all of southern and eastern China, Indonesia, Malaysia, and the Philippines, g) southern Japan, h) high latitude northeastern Russia, and i) the northern and eastern coastal regions of Australia. Other areas are either less flood-prone, or generate less attention due to smaller human population density or connection to the outside world. Thus, a) floods in Alaska and much of Canada are not widely reported, b) western Mexico is not nearly as subject to flooding as is eastern Mexico, c) floods in parts of Scandinavia, eastern Europe and central Russia, and northern China are also not widely reported, d) northern Africa including the Sahara lacks reported flooding, e) there are few reports of flooding from some desert areas such as the western U.S., parts of South Africa and Australia, western India, most of the Arabian Peninsula, and Mongolia.

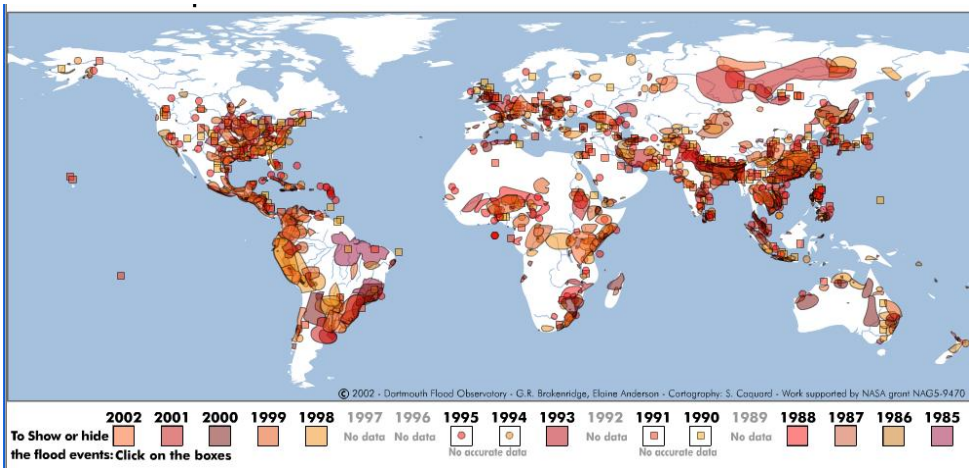

Figure 13. Global distribution of all floods, 1985-2002. Data from the Dartmouth Flood Observatory Active Archive of Floods (http://www.dartmouth.edu/~floods/archiveatlas/index.htm). Two years (1995 and 1996) are missing from this display.

Examination of the same reported floods, this time sorted by causation, also allows estimation of the dominant flood risk in different parts of the world. Figure 14, a-c and Figure 15, a-c, both provide global maps of the six most populous genetic classes of floods. In Figure 14, floods due to undifferentiated "heavy rain" are arrayed geographically approximately as per Figure 13; tropical storm-generated floods are common in: the southeastern U.S., Central America, southeastern Mexico, the Caribbean, Madagascar, southeastern Africa, southeast Asia, China, southern Japan, northern Australia, the Philippines, and Manchuria; and floods due to monsoonal rain occur primarily in India, China, Indochina, the Philippines, Indonesia, Malaysia, and northern Australia (seasonal high rainfall periods and flooding in some other regions will share some of the same monsoon genetic mechanisms).

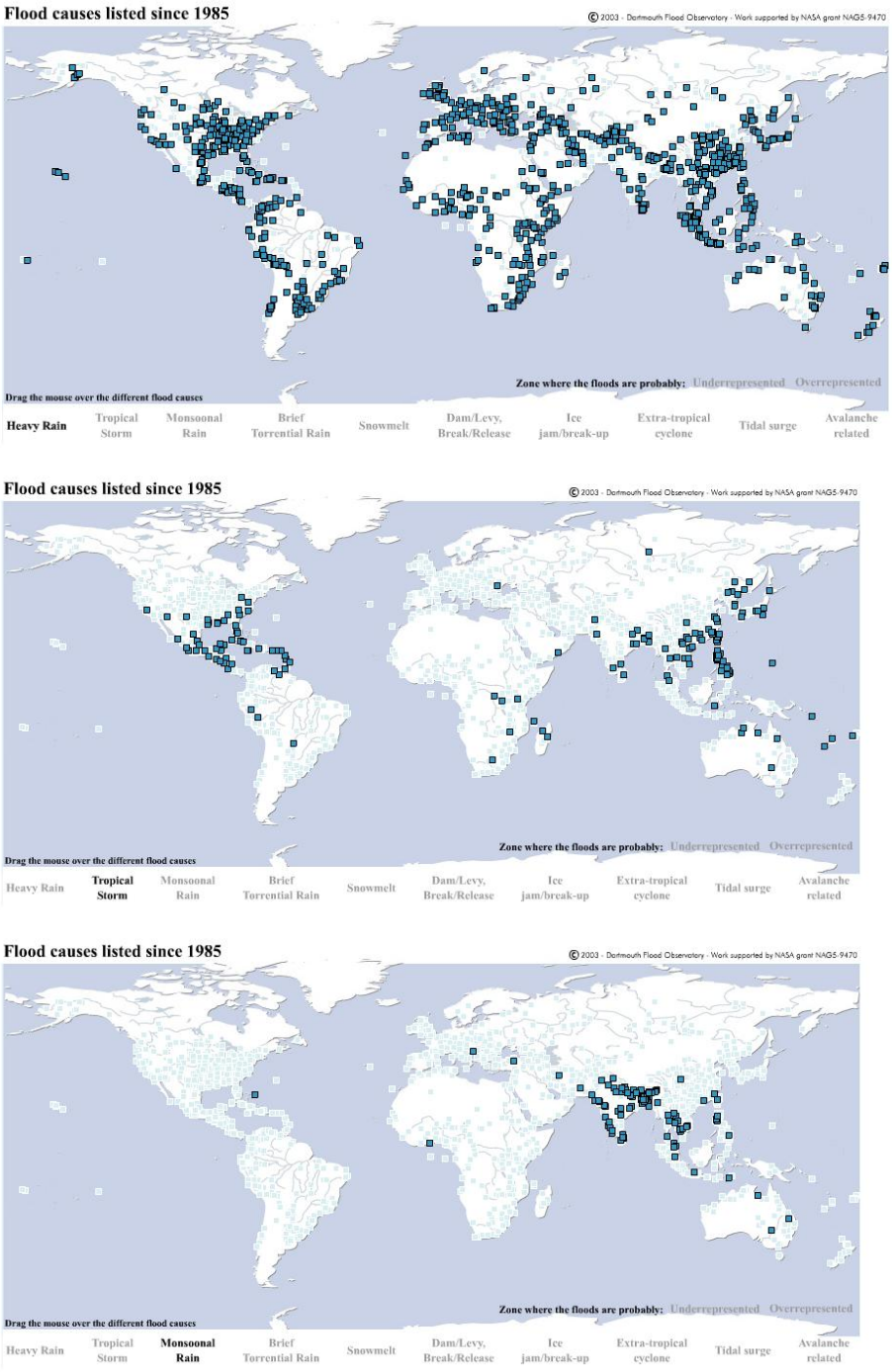

Figure 14, a., Area-affected centroid locations for cataloged floods from undifferentiated heavy rain, b., from tropical storm incursions, and c., from exceptionally intense monsoonal rains.

In Figure 15, floods due to brief torrential rains (often associated with flash flooding) exhibit a global geographic distribution somewhat similar to that in Figure 13. However, they are most common in the upland areas of Central America, northern South America, southeastern South America, Europe, Asia,

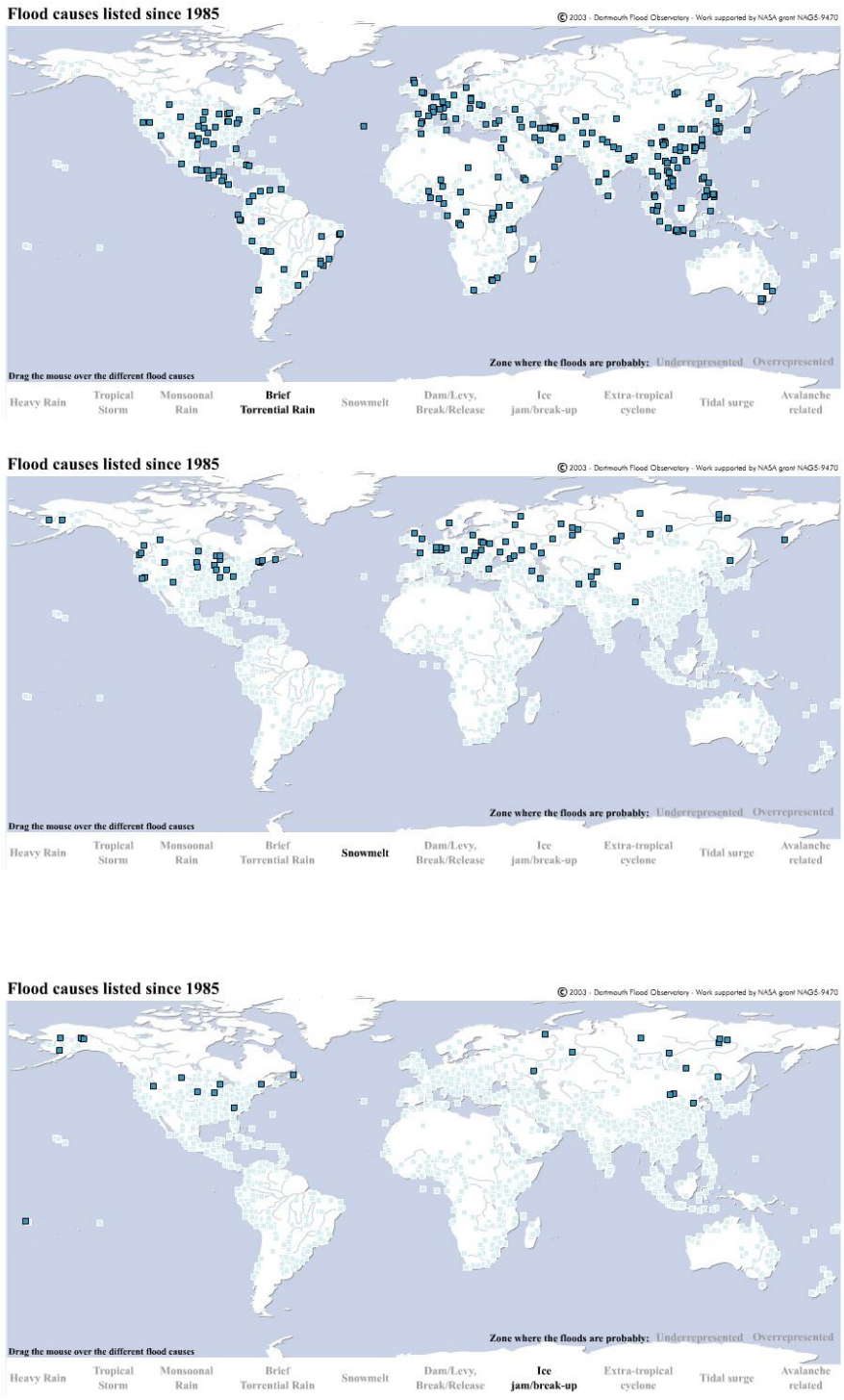

Figure 15. a., Area-affected centroid locations for cataloged floods from brief torrential rains, b., from snowmelt, and c., from ice jam break-ups.

Indonesia, Malaysia, the Philippines, Africa, and Australia. They also are common in the Midwestern U.S., where mesoscale convective storms during the summer months occur and extend over large areas. Floods due to snowmelt and to ice jams and ice jam breakups are, as expected, primarily affecting higher latitude northern hemisphere locations in Alaska, the northern U.S., and the north-flowing drainages of

central and northern Asia. The patterning of snow- and ice-related flooding in Canada and perhaps Scandinavia may not be well-represented due to under-reporting.

In turn, the causation of flooding affects the season of occurrence (Figures 16, a-c, and 17, a-c). These

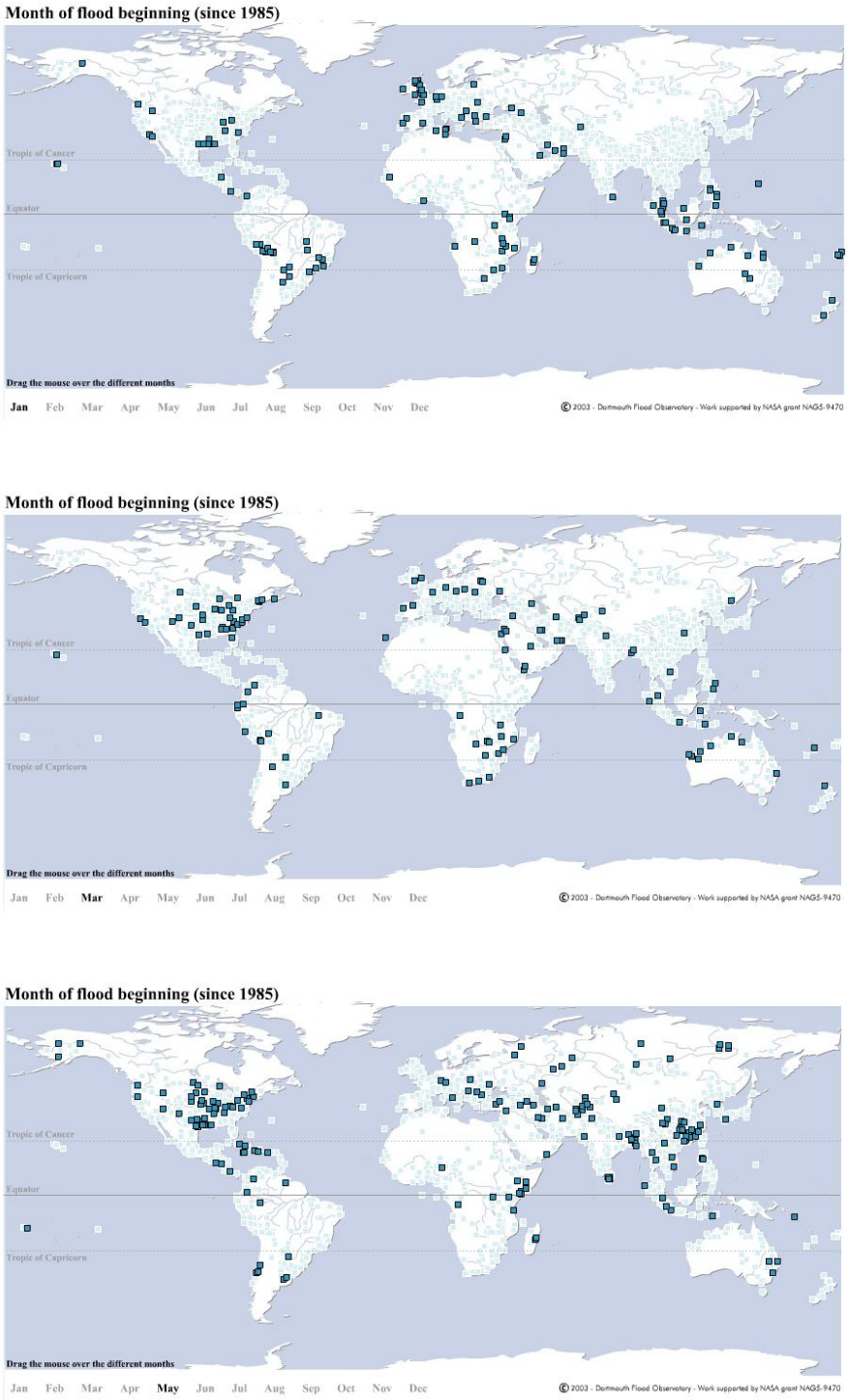

Figure 16. a., Area-affected centroid locations for cataloged floods in January, b., in March, and c., in May.

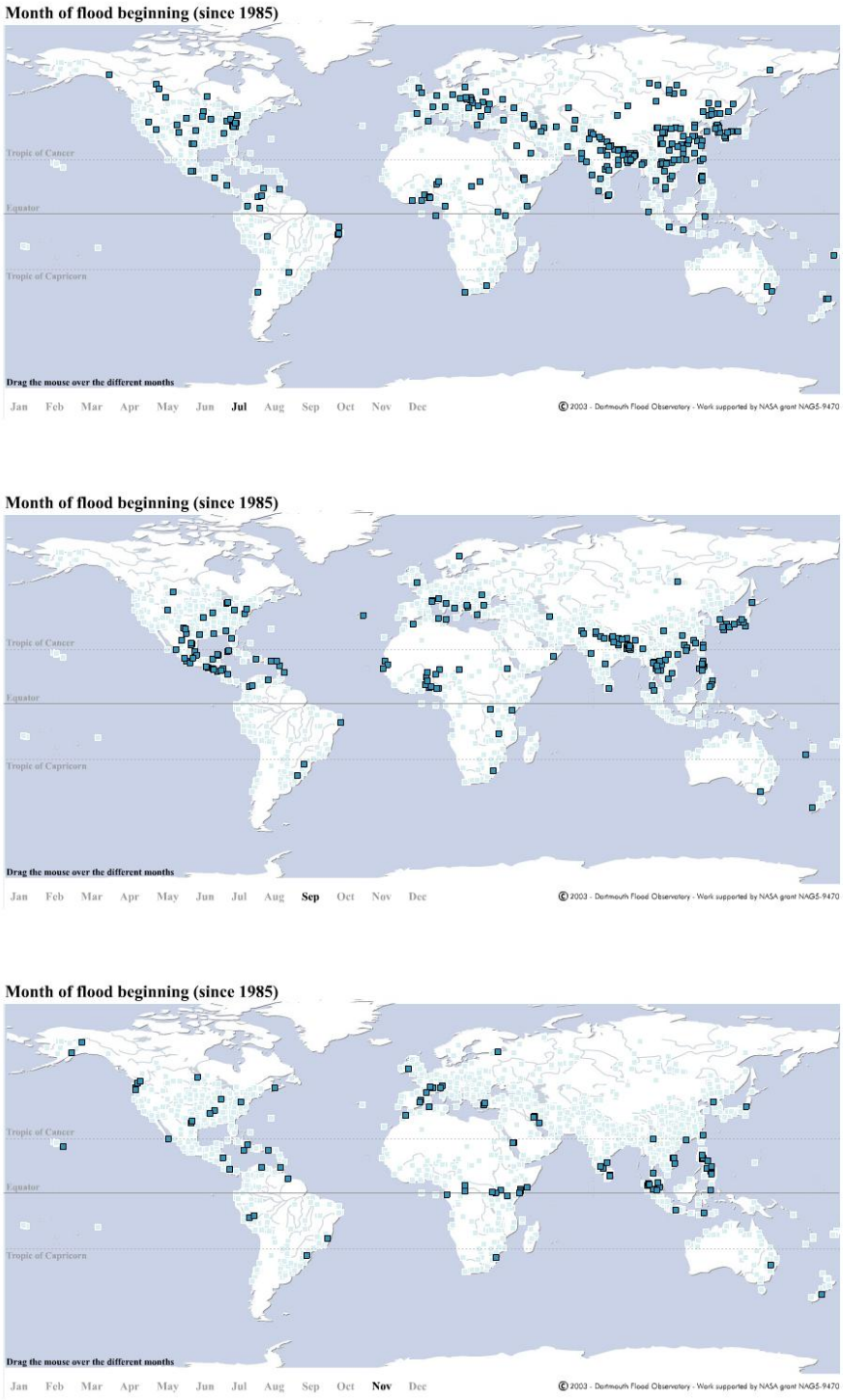

Figure 17. a., Area-affected centroid locations for cataloged floods in lllJuly, b.,in September, and c., in November.

maps (and other monthly maps, not shown) illustrate a global maximum (number of floods/month) during the northern summer, a concentration of flooding at northern low latitudes during late August and September, a December-May southern hemisphere maximum, a transition in the area affected by

flooding: from Asia, during the summer and late summer monsoon, to the south, from December to April/May, and a northern transition of African flooding in March-September coupled by a return southward migration in October-February.

In detail, the maps also illustrate the strong seasonality of flooding in many regions. For example, compare the number of events in each monthly map for: Indochina and the Philippines (summer brings both monsoonal rains and tropical storms), portions of India (exceptionally flood-prone in July), China (nearly flood-free in winter, progressing to yearly monsoon-related floods in July), South America, northwestern Australia and southeastern Africa (floodprone during January-March).

Strong seasonality of flooding may also be matched by a strongly bimodal "normal" streamflow distribution: rivers with seasonal flow regimes, such as within monsoonal lands, exhibit an annual "flood" season (e.g. figures 8 and 11), to which local agriculture has adjusted. As for stream gauging, remote sensing can record this normal annual cycle of surface water variation. If carried out in a consistent manner over a sufficient period of time, it can accurately distinguish zones of normal annual inundation from those affected by unusual high water. For example, in areas strongly affected by an annual monsoon (Figure 14c), agricultural insurers require not only information such as definition of the 10%, 5%, or 1 % exceedance probability floodplain, but also definition of the land affected by the mean annual flood. Accounting for unusual low-water years, this may be the land with a 75% exceedance probability of flooding each year, or a 1.33 average recurrence interval. Annual flooding is normal in such regions, where rivers exhibit a large seasonal variation and a relatively short period of high water each year. Flood risk assessment and flood damage indices should, therefore, focus on land above such normally flooded lands and on unusual damage to crops within the annual floodplain during years of severe flooding (larger-than-normal water depths and duration).

The combined information offers a path forwards towards the development of crop-specific flood damage indices. In particular, floods can be classified according to their genetic mechanism, seasonality, and geographic areas affected. For the important class of tropical storm floods, for example, the land areas affected by flooding can be delineated by the known history of tropical storm tracks (Figure 18).

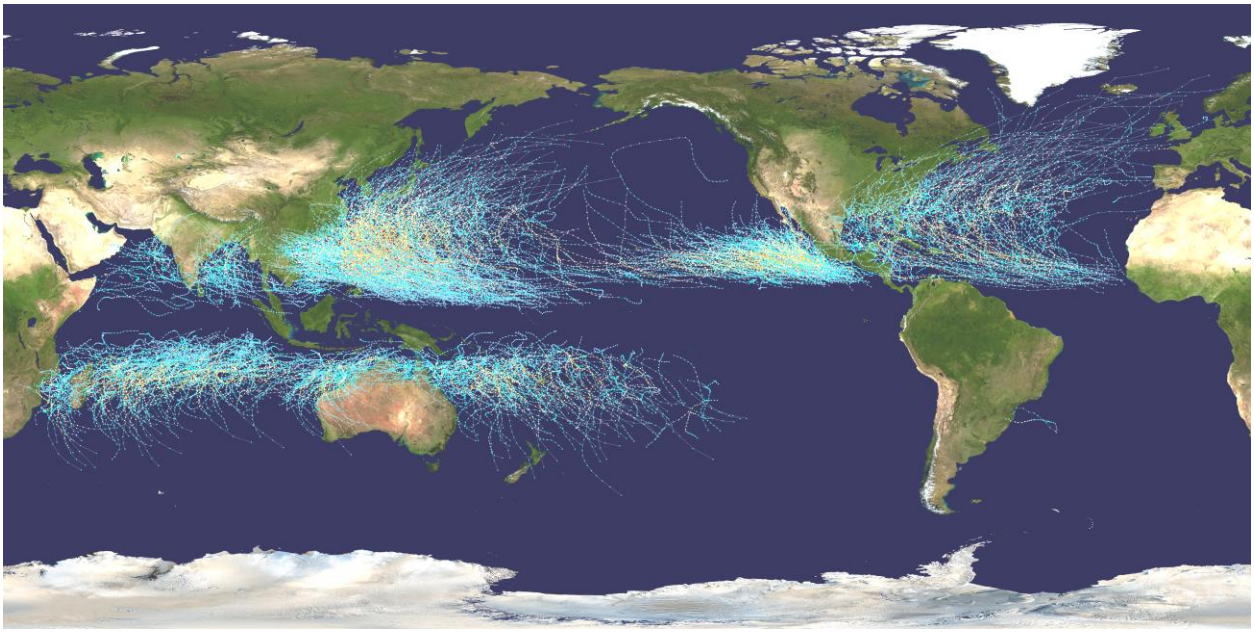

Figure 18. Twentieth Century tropical storm tracks compiled by the U.S. National Weather Service. (ref. to be added).

As summarized by the U.S. National Weather Service, the dates associated with the storm track data show that:

1) In the North Atlantic Ocean, a distinct hurricane season occurs from June 1 to November 30, sharply peaking from late August through September.
2) The northeastern Pacific Ocean has a broader period of activity, but in a similar time frame to the North Atlantic.
3) The northwestern Pacific sees tropical cyclones year-round, with a minimum in February and March and a peak in early September.
4) In the northern Indian Ocean, storms are most common from April to December, with peaks in May and November.
5) In the southern hemisphere, tropical cyclone activity begins in late October and ends in May. Southern Hemisphere activity peaks in mid-February to early March.

According to the considerations described above, and as demonstrated by Hirschbock (1988) and other workers, flood time series analysis can and should be responsive to the various flood-producing mechanisms within each watershed, and instead of regarding all floods as one population. Within Mozambique, for example, the most important type of severe flooding is induced by incursions of tropical storms far inland, and at particular times of the year (Figure 18). Such flooding exhibits its own probability distribution and seasonality, and remote sensing-assisted flood risk assessment can proceed by analysis of lands flooded, and flood discharges achieved, by these events as a class, rather than as part of a total time series including floods from disparate causes. This approach also allows an emphasis on those events most likely to be damaging to agriculture due to their season of their occurrence.

Summary and Conclusions

To be completed after reviewer input.

References Cited

Ali, S., Hassan, A., Martin, T. C., and Hassan, Q. K. (2001). Geospatial tools for monitoring floodplain water dynamics. *In* "Remote Sensing and Hydrology 2000." (M. Owe, K. Brubaker, J. Ritchie, and A. Rango, Eds.), pp. 465-471. IAHS, Oxford.

Arcement, G. J., and Schneider, V. R. (1989). Guide for selecting Manning's roughness coeffficents for natural channels and flood plains. *U.S. Geological Survey Water-Supply Paper 2339***,** 38p.

Archer, D. (1999). Practical application of historical flood information to flood estimation. *In* "Hydrological Extremes: Understanding, Predicting, Mitigating." (L. Gottschalk, J.-C. Olivry, D. Reed, and D. Rosbjerg, Eds.), pp. 191-199. IAHS Press, Institute of Hydrology, Wallingford, Wallingford, UK.

Arduino, G., Reggiani, P., and Todini, E. (2005). Recent advances in flood forecasting and flood risk assessment. *Hydrology and Earth System Sciences* **9,** 280-284.

Arnell, N. (1996). "Global Warming, river flows and water resources." John Wiley & Sons., NY.

Arnold, C. L., Boison, P. J., and Patton, P. C. (1982). Sawmill Brook: an example of rapid geomorphic change relating to urbanization. *Geological Society of America Bulletin* **90,** 155-166.

Bardossy, A., and Caspary, H. J. (1990). Detection of climate change in Europe by analyzing European atmospheric circulation patterns from 1881-1989. **42,** 155-168.

Barton, I., and Bathpls, J. (1989). Monitoring of floods with AVHRR. *International Journal of Remote Sensing* **10,** 1873-1892.

Bates, P. D., and Anderson, M. G. (1996). A preliminary investigation into the impact of initial conditions on flood inundation predictions using a time/space distributed sensitivity analysis. *Catena* **26,** 115-134.

Bates, P. D., Anderson, M. G., Baird, L., Walling, D. E., and Simm, D. (1992). Modeling floodplain flow with a two-dimensional finite element scheme. *Earth Surface Proceses and Landforms* **17,** 575-588.

Bates, P. D., Anderson, M. G., and Hervonet, J.-M. (1995). Initial comparison of two two-dimensional finite element codes for river flood simulation. *Proc. Inst. Civ. Engin. Wat. Marit. and Energy* **112,** 238-248.

Bates, P. D., and De Roo, A. P. J. (2000). A simple raster-based model for flood inundation simulation. *Journal of Hydrology* **236,** 54-77.

Bates, P. D., Horritt, M. S., Smith, C. N., and Mason, D. (1997). Integrating remote sensing observations of flood hydrology and hydraulic modeling. *Hydrological Processes* **11,** 1777-1795.

Bates, P. D., Marks, K. J., and Horitt, M. S. (2002). Optimal use of high-resolution topographic data in flood inundation models,. *Hydrological Processes* **17,** 537-557.

Beckman, E. W. (1976). Magnitude and Frequency of Floods in Nebraska. *U.S. Geological Survey Water Resources Investigation,* 76-109.

Betts, R. A., Boucher, O., Collins, M., Cox, P. M., Falloon, P. D., Gedney, N., Hemming, D. L., Huntingford, C., Jones, D., Sexton, M. H., and Webb, M. J. (2007). Projected increase in continental runoff due to plant responses to increasing carbon dioxide. *Nature* **448,** 1037-1041.

Blasco, F., Bellan, M. F., and Chaudhury, M. W. (1992). Estimating the extent of floods in Bangladesh using SPOT data. *Remote Sens. Environ.* **39,** 167-178.

Blasco, F., Fromard, F., and Chaudhury, M. U. (1989). Floods in Bangladesh. A preliminary study with SPOT 1 data. CNES, Paris.

Brakenridge, G. R., and Anderson, E. (2005). MODIS-based flood detection, mapping, and measurement: the potential for operational hydrological applications. *In* "Transboundary Floods: Reducing Risks Through Flood management, Proc. of NATO Advanced Research Workshop, Baile Felix – Oradea, Romania." (J. Marsalek, G. Stancalie, and G. Balint, Eds.), pp. 1-12. Springer-Verlag, Dordrecht, Netherlands.

Brakenridge, G. R., and Anderson, E. (2006a). Dartrmouth Flood Observatory Active archive of large floods, 1985-present. Dartmouth College, Hanover, NH USA.

Brakenridge, G. R., and Anderson, E. (2006b). World Atlas of Flooded Lands. *http://www.dartmouth.edu/~floods/Atlas.html*.

Brakenridge, G. R., Anderson, E., Nghiem, S. V., Caquard, S., and Shabaneh, T. (2002). Flood warnings, flood disaster assessments, and flood hazard reduction: the roles of orbital remote sensing. *In* "Proceedings of the 30th International Symposium on Remote Sensing of the Environment." pp. 4, Honolulu.

Brakenridge, G. R., Anderson, E., Nghiem, S. V., De Groeve, T., and Kugler, Z. (2007a). Microwave Sensing of Global River Runoff. *In* "Satellite Observation of the Global Water Cycle Workshop, University of California-Irvine and the Jet Propulsion Laboratory, California Institute of Technology." (J. Famiglietti, E. Njoku, S. Sorooshian, and D.Waliser, Eds.), University of California, Irving, CA.

Brakenridge, G. R., Nghiem, S. V., Anderson, E., and Mic, R. (2007b). Orbital Microwave Sensor Measurement of River Discharge and Ice Status. *Water Resources Research* **43,** doi:10.1029/2006WR005238.

Bronstert, A. (1995). River flooding in Germany: influenced by climate change? *Physics and Chemistry of the Earth* **20,** 445-450.

Burke, R. L. (1983). Computerized Agricultural Crop Flood Damage Assessment System. *ARMY ENGINEER DISTRICT, VICKSBURG MISS* **STINET ADP002639,** 10.

Burn, D. H., and Arnell, N. W. (1993). Synchronicity in global flood responses. *Journal of Hydrology* **144,** 381-404.

Byrne, G. F., Dabrowska-Zielinski, K., and Goodrick, G. N. (1981). Use of visible and thermal satellite data to monitor an intermittently flooding marshland. *Remote Sens. Environ.* **11,** 393-399.

Chuan, C. Y., and Jujn, L. h. (2003). An analysis of the variation of maximum flood stage of the Lower Yangtze River. *Journal of Hydraulic Research* **41,** 235-238.

De Groeve, T., Kugler, Z., and Brakenridge, G. R. (2007). Near real time flood alerting for the global disaster alert and coordination system. *Information Systems for Humanitarian Operations" session at ISCRAM (Information Systems for Crisis Response and Management), Delft, The Netherlands*.

Deutsch, M., and Ruggles, F. (1974). Optical data processing and applications of the ERTS-1 imagery covering the 1977 Mississippi River Valley floods. *Am. Wat. Res. Assoc. Water Res. Bull* **10,** 1023-1039.

Dingman, S. L. (1994). "Physical Hydrology." Prentice-Hall Inc., Englewood Cliffs, NJ.

Farr, T. G., and al., e. (2007). The Shuttle Radar Topography Mission. *Rev.*
Geophys. Res. Lett. **45**.

Few, R., Ahern, M., Matthies, F., and Kovats, S. (2004). Floods, health, and climate change: a strategic review. *In* "Working Paper 63." Tyndal Centre For Climate Change Research.

Franks, S. W., and Kuczera, G. (2002). Flood frequency analysis: evidence and implications of secular climate variability, New South Wales. *Water Resources Research* **38,** 1062.

French, J. R. (2003). Airborne LiDAR in support of geomorphological and hydraulic modelling. *Earth Surface Proceses and Landforms* **28,** 321-335.

Gumley, L., and King, M. D. (1995). Remote sensing of flooding inthe U.S. Upper Midwest during the summer of 1993. *Bulletin of the American Meteorological Society* **76,** 933-943.

Guowei, L., and Jingping, W. (1999). A study of extreme floods for China for the past 100 years. *In* "Hydrological Extremes: Understanding, Predicting, Mitigating." (L. Gottschalk, J.-C. Olivry, D. Reed, and D. Rosbjerg, Eds.), pp. 109-119. IAHS Press, Institute of Hydrology, Wallingford, Wallingford, UK.

Halcrow-Group-Ireland-Ltd. (2007). Lee Catchment Flood Risk Assessment and Management Stud. **http://www.leecframs.ie/floodsdirective.asp**.

Harris, A. R., and Mason, I. M. (1989). Lake area measurement using AVHRR. *International Journal of Remote Sensing* **10,** 885-895.

Heiler, H., Hein, T., Schiemer, F., and Bornette, G. (1995). Hydrological connectivity and flood pulses as the central aspects for the intergrity of a river-floodplain system. *Regulated Rivers* **11,** 351-361.

Hess, L. L., Melack, J. M., and Simonett, D. S. (1990). Radar detection of flooding beneath the forest canopy: a review. *Int. J. Remote Sens.* **11,** 1313-1325.

Hirschboeck, K. K. (1988). Flood hydroclimatology. *In* "Flood Geomorphology." (V. R. Baker, R. C. Kochel, and P. C. Patton, Eds.), pp. 27-49. John Wiley & Sons.

Hlacova, K., Kohnoya, S., Kubes, R., Szolgay, J., and Zvlonsky, M. (2005). Estimation of future flood risk for flood warning systems. *Hydrology and Earth System Sciences* **9,** 153-170.

Hutchinson, C., Drake, S., van Leeuwen, W., Kaupp, V., and HaithcoaT. (2003). Characterization of PECAD's DSS: a zeroth-order assessment and benchmarking preparation. *Report commissioned by NASA HQ, Washington DC, and prepared by University of Arizona and University of Missouri*.

Islam, M. M., and Sado, K. (2000). Flood hazard assesment in Bangladesh using NOAA AVHRR data with geographical information system. *Hydrological Processes* **14,** 605-620.

Islam, M. M., and Sadu, K. (2000a). Development of flood hazard maps of Bangladesh using NOAA-AVHRR images with GIS. *Hydrological Science Journal* **45,** 605-620.

Islam, M. M., and Sadu, K. (2000b). Flood hazard assessment in Bangladesh using NOAA-AVHRR data with geographical information system. *Hydrological Processes* **14,** 605-620.

Karnes, D., and Brakenridge, G. R. (1998). The Dartmouth Flood Observatory: an electronic research tool and archive for investigations of extreme flood events. *Geoscience Information Society Special Publication*.

Katz, R. W., and Brown, B. G. (1992). Extreme events in a chaning climate: variability is more important than averages. *Climate Change* **21,** 289-302.

Kiesiel, C. C. (1969). Time series analysis of hydrologic data. *Advances in Hydrosciences* **5,** 1-119.

Knox, J. C. (1985). Responses of floods to Holocene climatic change in the Upper Mississippi Valley. **23,** 287-300.

Knox, J. C. (1993). Large increases in flood magnitude in response to modest changes in climate. *Nature* **430-432**.

Komuscu, A. L., Ayhan, E., and Celik, S. (1998). Analysis of meteological and terrain features leading to the Izmir flash flood, 3-4 November 1995. *Natural Hazards* **18,** 1-25.

Kugler, Z., De Groeve, T., Brakenridge, G. R., and Anderson, E. (2007). Towards a near-real time global flood detection system (GFDS). *The International Archives of the Photogrammetry, Remote Sensing and Spatial Information Sciences, , Davos* **10th Intl. Symposium on Physical Measurements and Signatures in Remote Sensing,** 10.

Liu, Z. L., and Liu, N. (2002). Flood area and damage estimation in Zhejiang, China. *Journal of Environmental Management* **66,** 1-8.

McDowell, M. (2002). Melting ice triggers Himalayan flood warning. *Nature* **416,** 776.

McGinnis, D. F., and Rango, A. (1975). Earth Resources Satellite System for flood monitoring. *Geophysical Research Letters* **2,** 132-135.

Merabtene, T., and Yoshitana, J. (2005). Technical Report on Global Trends of Water-related Disasters. *In* "Technical Memoradum of Public Works Research Institute." pp. 124, 1-6 Minamihara, Tsukuba-Shi, Japan.

Mertes, K. A. K. (1997). Documentation and significance of the perirheic zone on innundated floodplains. *Water Resources Research* **33,** 1749-1762.

Mertes, L. A. K. (1990). "Hydrology, hydraulics, sediment transport, and geomorphology of the central Amazon flodplain." Ph.D. Dissertation, University of Washington, Seattle.

Mertes, L. A. K., Daniel, D. I., Melack, J. M., Nelson, B., Martinelli, L. A., and Forsberg, B. R. (1995). Spatial patterns of hydrology, geomorphology, and vegetation on the floodplain of the Amazon River in Brazil from a remote sensing perspective. *Geomorphology* **13,** 215-232.

Miller, J. M., and Osterkamp, T. E. (1978). The use of Landsat data to minimize flooding risks caused by ice jams in Alaskan Rivers. *In* "Proc. of the 12th International Symposium on Remote Sensing of Environment." pp. vol. 3: 2255-2266, Environmental Research Institute of Michigan (ERIM), Ann Arbor, Michigan USA.

Milly, P. C. D., Weatherald, R. T., Dunne, K. A., and Delworth, T. L. (2002). Increasing risk of great floods in a changing climate. *Nature* **415,** 514-517.

Mitchell, J. K., and Ericksen, N. J. (1992). Effects of climatic change on weather-related disasters. *In* "Confronting Climate Change: Risks, Implications and Responses." (I. M. Mintzer, Ed.), pp. 141-151. Cambridge University Press, Cambridge.

Moore, G. K., and North, G. W. (1974). Flood inundation in the southeaster United States from aircraft and satellite imagery. *Am. Wat. Res. Assoc. Water Res. Bull.* **10,** 1082-1096.

Nico, G., Pappalepore, M., Pasquariello, G., Refice, A., and Samarelli, S. (2000). Comparison of SAR amplitude versus coherence flood detection methods-A GIS application. *International Journal of Remote Sensing* **21,** 1619-1631.

Njoku, E. G., Ashcroft, P., Chan, T. K., and Li, L. (2005). Global survey and statistics of radio-frequency interference in AMSR-E land observations. *IEEE Trans. Geosci. Remote Sens* **43,** 938-947.

Njoku, E. G., and Chan, S. (2006). Vegetation and surface roughness effects on AMSR-E land observations. *Remote Sensing of the Environment* **100,** 190-199.

Njoku, E. G., T. J. Jackson, V. Lakshmi, Chan, T. K., and Nghiem., S. V. (2003). Soil moisture retrieval from AMSR-E. *IEEE Trans. Geosci. Remote Sens* **41,** 215-229.

Okimoto, K., Yamakawa, S., and Kawashima, H. (1998). Estimation of flood damage of North Korea in 1995. *International Journal of Remote Sensing* **19,** 365-371.

PASCO. (2006). Earth observation-based multi-periil crop index development for agricultural insurance-product development study. *Unpublished Technical Report*.

Pinter, N., and Heine, R. A. (2005). Hydrodynamic and morphodynamic response to river engineering documented by fixed-discharge analysis, Lower Missouri River, USA. *Journal of Hydrology* **302,** 70-91.

Pinter, N., Thomas, R., and Wlosinski, J. H. (2001). Flood-hazard assessment on dynamic rivers. *Eos: Transactions of the American Geophysical Union* **82,** 333-333.

Pinter, N., Thomas, R., and Wlosinski, J. H. (2002a). Reply to U.S. Army Corps of Engineers Comment on "Assessing flood hazard of dynamic rivers. *EOS, Trans. American Geophysical Union* **83,** 397-398.

Pinter, N., Wlosinski, J. H., and Heine, R. (2002b). The case for utilization of stage data in flood-frequency analysis: preliminary result from the Middle Mississipp and Lower Mississippi River. *Hydrologic Scence and Technology Journal* **18,** 173-185.

Profeiti, G., and MacIntosh, H. (1997). Flood management through Landsat TM and ERS SAR data: a case study. *Hydrological Processes* **11,** 1397-1408.

Quan, W., Watanabe, M., Hayashi, S., and Murakami, S. (2003). Using NOAA AVHRR data to assess flood damage in China. *Environmental Monitoring and Assessment* **82,** 119-148.

Rango, A., and Salomonson, V. V. (1974a). Flood hazard studies in the Mississippi Basin using remote sensing. *Water Resources Bulletin* **10,** 1060-1081.

Rango, A., and Salomonson, V. V. (1974b). Regional flood mapping from Space. *Water Resources Research* **10,** 473-484.

Rasid, H., and Pramanik, M. A. H. (1993). Areal extent of the 1988 flood in Bangladesh: how much did the satellite imagery show? *Natural Hazards* **8,** 189-200.

Reed, D., Doerte, J., Robson, A. J., Faulkner, D. S., and Stewart, E. J. (1999). Regional frequency analysis: a new vocabulary. *In* "Hydrological Extremes: Understanding, Predicting, Mitigating." (L. Gottschalk, J.-C. Olivry, D. Reed, and D. Rosbjerg, Eds.), pp. 237-243. IAHS Press, Institute of Hydrology, Wallingford, Wallingford, UK.

Robinove, C. J. (1978). Interpretation of a Landsat image of an unusual flood phenomenon in Australia. *Remote Sens. Environ.* **7,** 219-225.

Rosenqvist, A., Forsberg, B. R., Pimentel, T., Rauste, Y. A., and Riche, J. E. (2002). The use of spaceborne radar data to model inundation patterns and trace gas emission in the central Amazon flood plain. *International Journal of Remote Sensing* **23,** 1303-1328.

Sanders, R., Shaw, F., MacKay, F., Galy, H., and Peterk, O. (2005). National flood modeling for insurance purposes using IFSAR for flood risk estimation in Europe. *Hydrology and Earth System Sciences* **9,** 22-34.

Sheng, Y., Su, Y., and Xiao, Q. (1998). Challenging the cloud-contamination problem in flood monitoring with NOAA/AVHRR imagery. *Photogrammetric Engineering and Remote Sensing* **64,** 191-198.

Simpson, C. J., and Doutch, H. F. (1977). The 1974 wet season flooding of the southern Carpentaria Plains, northwest Queensland. *Bur. Min. Res. Jour. of Australian Geology and Geophysics* **2,** 43-51.

SIWRP. (2006). HYDROLOGICAL RISK ZONE MAPPING IN DONG THAP PROVINCE. *Southern Institute for Water Resources Planning Technical Report,* 51.

USGS. (1993). Nationwide summary of US Geological Survey regional regression equations for estimating magnitude and frequency of floods for ungaged sites (U. S. G. Survey, Ed.).

Verma, B. N. (1997). Flood Devastation and Agricultural Development in Eastern India. *Proceedings of a National Seminar on Flood Devastation and Development in Eastern India, 28-29 November 1997, Department of Agricultural Economics, Rajendra Agricultural University, Pusa, Samastipur, Bihar*.

Wentz, F. J., Ricciarduilli, L., Hilburnj, K., and Mears, C. (2007). How much more rain will global warming bring? *Nature* **317,** 233-235.

Wiesnet, D. R., McGinnis, D. F., and Pritchard, J. A. (1974). Mapping of the 1973 Mississippi River floods by the NOAA-2 satellite. *Water Resource. Bull.* **10,** 1040-1049.

Wilshire, S. E. (1986). identification of homogenous regions for flood frequency analysis. *Journal of Hydrology* **84,** 387-402.

Yamagata, Y., and Akiyama, T. (1988). Flood damage analysis using multitemporal Landsat Thematic Mapper data. *Int. J. Remote Sens.* **9,** 00.

Zhang, X. B., Zwiers, f. W., Heggerl, G. C., Lambert, F. H., Gillett, N. P., Solomon, S., Stott, P. A., and Nozawa, T. (2007). Detection of human influence on twentieth-century precipitation trends. *Nature* **448,** 461-465.